



Annual Report 2022

The world's leading facility in neutron science & technology





Annual Report 2022
Institut Laue-Langevin



Contents

Publishing information

EDITORS:
Giovanna Cicognani and Jacques Jestin

PRODUCTION TEAM:
Giovanna Cicognani and Virginie Guerard

DESIGN:
Morton Ward Limited

PHOTOGRAPHY:
ILL (unless otherwise specified)
Cover: © L. Thion

Further copies can be obtained from:
Institut Laue-Langevin
Communication Unit
CS 20156, F-38042 Grenoble Cedex 9

 communication@ill.eu

 www.ill.eu

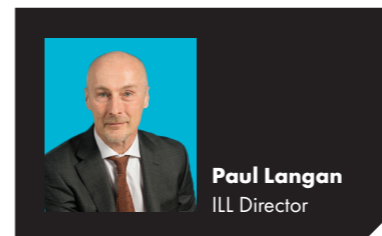
▶ DIRECTOR'S FOREWORD	5	▶ INDUSTRIAL USE	42
▶ WHAT IS THE ILL	6	▶ MORE THAN SIMPLY NEUTRONS	46
This is the ILL	7	Scientific support laboratories	48
Why neutron scattering is useful	7	Training and outreach	50
▶ SCIENTIFIC HIGHLIGHTS	8	▶ WORKSHOPS AND EVENTS	52
Highlights introduction	10	▶ FACTS AND FIGURES	56
Colleges' introduction	12	Facts and figures	58
Scientific highlights	14	Publications	61
▶ FACILITY UPDATE	30	Organisation chart	62
The ILL 20-23 programme	32		
Endurance gain matrix	34		
Instrument list and layout	36		
Timeline long shutdown works	38		

As one of the world's leading research institutions, ILL has played a key role in many fields of science over the last 50 years.



Foreword

© L. Thion



Paul Langan
ILL Director

At the ILL, we typically schedule major work to maintain and improve our research facility during extended periods of reactor shutdown, whilst maximising the numbers of neutron days available for visiting researchers in between these shutdowns. In 2022 our primary focus was on successfully completing the carefully planned programme of work for the latest extended reactor shutdown, which we refer to as the H1–H2 shutdown. The H1–H2 shutdown began in October 2021 and ended in February 2023, only a few days later than originally scheduled. Given the complexity, intensity and interdependence of the work carried out, this can be regarded as a major success. I also see it as a testament to the skill and commitment of ILL staff. What we have achieved in 2022 positions the ILL, with its new and upgraded neutron science capabilities, as a safe, secure and sustainable reactor.

H1–H2 is a double beam tube that extracts thermal and cold neutrons from the reactor reflector and channels them through multiple neutron guides to all the instruments in the ILL7 guide hall. Of all the ILL beam tubes, H1–H2 is the most important. That is because half the entire suite of ILL instruments is located in ILL7. H1–H2 has to be replaced because of irradiation embrittlement—it was last changed in 2005. At the same time, an important part of the infrastructure of the neutron guides was also replaced. Furthermore, several instruments were upgraded and new instruments constructed in ILL7 and in other areas of the facility, as part of the last phase of the ENDURANCE programme. In this 2022 annual report you can read about these projects and the many other important maintenance and improvement tasks that were completed during the shutdown.

Another important achievement in 2022 was a review of the scientific performance of all ILL instruments and user support activities by an external committee of

experts from across the world. The review, commissioned by the Scientific Council, concluded that the ILL has a world-class suite of instruments, some of which are world-leading and unique. It also provided a rich set of data that will help the ILL optimise experimental capabilities within the envelope of available resources. In particular, one result is the identification of instruments that will be fully or partially removed from the user programme as new instruments with new experimental capabilities are introduced. This review represents a cornerstone for future strategic development at the ILL. It shows the way forward in terms of providing visiting researchers with the best possible neutron science capabilities that available resources allow.

With the reactor not in operation, 2022 was the ideal opportunity for ILL scientists to engage with user communities in our eleven Scientific Member countries as well as with prospective new member countries. Collectively, our Scientific Members provide about one quarter of the ILL's budget and are responsible for a corresponding proportion of high-quality scientific output. Discussions are underway to ensure the ongoing, highly valued support of Members through the 6th Protocol period (2024–33), which was approved by our Associates in September 2021.

Finally, the financial environment in 2022 was difficult for many user facilities in Europe because of rising costs for electricity and materials. The ILL was no exception. However, we also faced additional challenges with unanticipated costs associated with new safety and security requirements. Over the course of the year we planned and took action to mitigate the impact of cost increases in order to ensure the long-term financial security and viability of the Institute. We are grateful for the additional funds that Associate countries France, Germany and the UK gave us to help with these challenges.

At this point in time, early 2023, we greatly look forward to restarting the reactor so that we continue with our primary mission of providing visiting European researchers access to a world-class suite of neutron instruments with new and upgraded experimental capabilities. After all the hard work during the H1–H2 shutdown, it is time to enter a phase of delivering science for the decade to come. The ILL has never been better positioned to apply its powerful capabilities to making new scientific discoveries and solving critical research problems. The challenge now, is to seize this window of opportunity so that we make a difference and improve human welfare by tackling major challenges in health, climate, the environment and new materials.

“2022 saw an extremely intensive programme of work at ILL – one of the richest and most complex the Institute has ever seen. This extraordinary accomplishment will extend the boundaries of science at ILL over the next ten years.”

Maria Faury
Chair of the ILL Steering Committee in 2022

What is the ILL?



This is the ILL

The Institut Laue Langevin (ILL) is an international research centre providing world-leading facilities in neutron science and technology. Neutrons are used at the ILL to probe the microscopic structure and dynamics of a broad range of materials at molecular, atomic and nuclear level.

The ILL operates the most intense neutron source in the world, a 58.3 MW nuclear reactor designed for high brightness. The reactor normally functions round-the-clock for three to four 50-day cycles per year, burning a single, highly enriched uranium fuel element with very low radioactive waste and effluents. The reactor supplies neutrons to a suite of 40 high-performance instruments constantly maintained at the highest state of the art.

The ILL is owned by its three founding countries—France, Germany and the UK. These three Associate countries contributed some 78 M€ to the Institute in 2022, a sum enhanced by significant contributions from the ILL's Scientific Member countries: Austria, Belgium, the Czech Republic, Denmark, Italy, Poland, Slovakia, Slovenia, Spain, Sweden and Switzerland. The ILL's overall budget in 2022 amounted to about 108 M€.

As a service institute, the ILL makes its facilities and expertise available to visiting scientists. It has a global user community of about 2 000 researchers from almost 40 countries who come to work at the ILL every year. The 850 experiments they perform annually are pre-selected by a scientific review committee. Between 550 and 600 scientific papers are published annually, following the treatment and interpretation of data obtained from the use of our facilities. Of these articles, 145 were published in high-impact journals in 2022.

Neutrons and society

The scope of the research carried out at the ILL is very broad, embracing condensed-matter physics, chemistry, biology, materials and earth sciences, engineering, and nuclear and particle physics. Much of it impacts on many of the challenges facing society today, from sustainable sources of energy, better healthcare and a cleaner environment, to new materials for information and computer technology.

Much of the research carried out at the ILL impacts on many of the challenges facing society today.

Preparing for the future

To maintain its status as leader in neutron science, the Institute has constantly upgraded its instruments, infrastructure and scientific equipment over the last 50 years. The latest modernisation programme—Endurance—was launched in 2016 and is currently in its second phase (2020–2023). When completed, the Endurance programme will offer new possibilities in the fields of magnetism, materials science, soft matter, biology and particle physics, with a view to maintaining the Institute's world-leading position for another decade at least.

Why neutron scattering is useful

When used to probe small samples of materials, neutron beams have the power to reveal what is invisible using other forms of radiation. Neutrons can appear to behave as particles, waves or microscopic magnetic dipoles; with these very specific properties they can provide information that is often impossible to obtain using other techniques. Below are a few of the special characteristics of neutrons.

Wavelengths of tenths of nanometres

Neutrons have wavelengths varying from 0.01 to 100 nanometres. This makes them an ideal probe into atomic and molecular structures whether composed of single atomic species or complex biopolymers.

Energies of milli-electronvolts

The milli-electronvolt energies associated with neutrons are of the same magnitude as the diffusive motions of atoms and molecules in solids and liquids, the coherent waves in single crystals (phonons and magnons) and the vibrational modes in molecules. Therefore, any energy

exchange of between 1 μeV (or even 1 neV with neutron spin-echo techniques) and 1 eV between the incoming neutron and the sample is easy to detect.

Microscopically magnetic

Neutrons possess a magnetic dipole moment, which makes them sensitive to the magnetic fields generated by unpaired electrons in materials. They therefore play an important role in investigations of the magnetic behaviour of materials at the atomic level. In addition, as the neutron scattering effect of the atomic nuclei in a sample depends on the orientation of the spin of both the neutron and the atomic nuclei, neutron scattering techniques are ideal for detecting nuclear spin order.

Electrically neutral

As neutrons are electrically neutral they can penetrate far into matter without doing damage. They are therefore precious allies in research into biological samples or engineering components under extreme conditions of pressure, temperature or magnetic field, or within chemical-reaction vessels.

High sensitivity and selectivity

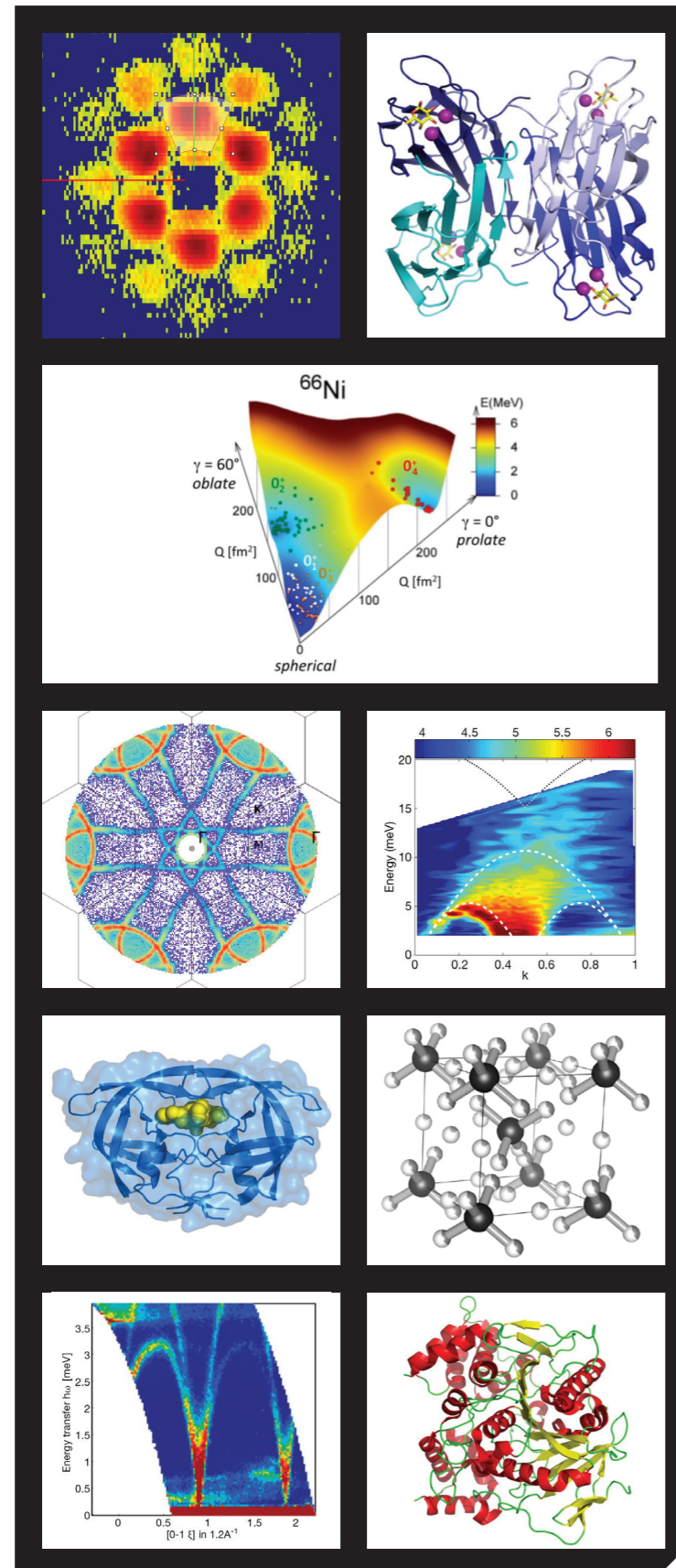
The scattering from nucleus to nucleus in a sample varies in a quasi-random manner, even for different isotopes of the same atom. This means that light atoms remain visible in the presence of heavy atoms and atoms close to each other in the periodic table can be clearly distinguished. This makes it possible to use isotopic substitution in order to vary the contrast in certain samples and thus highlight specific structural features. Neutrons are also particularly sensitive to hydrogen atoms and are therefore essential for research into hydrogen-storage materials, organic molecular materials and biomolecular samples or polymers.



Scientific highlights

© L. Thion

The ILL – leader in neutron research for the next decade



Neutron techniques are vital research tools in science and innovation. They help us to understand and develop better materials to tackle major societal challenges. Over the years, advances in instrumentation have continuously improved signal quality and reduced sample requirements (size and composition), opening up fundamentally new research opportunities.

The ILL has been the world's neutron flagship facility for more than 50 years, successfully adapting to the ever-changing science and innovation landscape. This has been possible thanks to our continuous investment in scientific equipment and infrastructure, meaning that many of the world's best instruments can now be found in one comprehensive suite.

The latest ILL modernisation programme, **Endurance**, was launched in 2016. With a total investment of 60 M€, it was scheduled to be rolled out in two phases over eight years. Running in parallel with a major programme of maintenance, security and safety work on the reactor, it has entailed upgrades to instruments, infrastructure and guides (ILL20–23 programme, see p32).

As a result, after a 16-month reactor shutdown throughout the whole of 2022, and with Endurance close to completion, the ILL User Programme restarted in March 2023 with an unequalled suite of state-of-the-art neutron instruments.

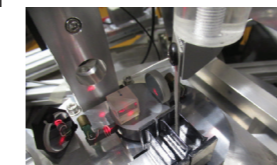
With improved signal quality and new sample environment equipment, the range of experimental conditions offered to users will broaden. Kinetics experiments with finer time resolution will give new insight into time-dependent processes; and increasing ranges in temperature, pressure and magnetic and electric fields will enable experiments under ever more extreme conditions. Taken together, these developments will enable scientists to study more complex technological and bio-materials during processing, synthesis and *operando* conditions, giving them the ability to tailor their properties at the nanoscale.

The Endurance instrument projects will also offer unprecedented capabilities in terms of flux, resolution, flexibility and sample environment. These will allow users to perform highly innovative experiments in many scientific areas—from the study of sustainable sources of energy and ground-breaking research for health, to the development of new quantum materials for information and computing technology.

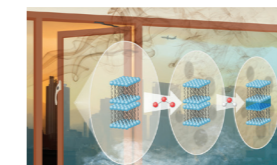
The following college introductions and research highlights presented in this section demonstrate the many ways in which the ILL can and will help to tackle major societal challenges of our times.

Visit our web pages to discover our recent science highlights:

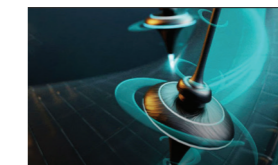
<https://www.ill.eu/news-press-events/news/recent-highlights>



A quantum way in two crystals.



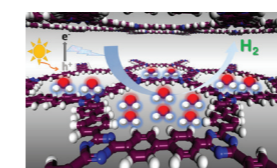
Grimy windows could be harbouring toxic pollutants.



One step closer to quantum and magnonic devices.



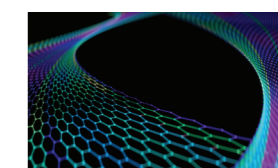
New technique reveals how bacteria initiate infection.



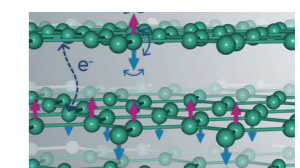
Investigating the secrets of greener hydrogen fuel production.



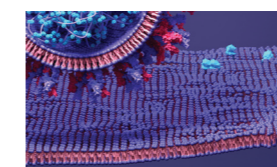
A superior treatment for cancer.



The case of the curious superconductor.



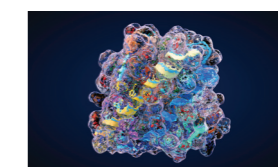
Putting the pressure on magnetism.



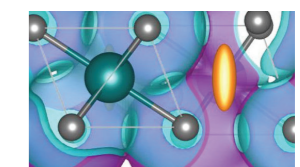
Understanding the lipid bilayer degradation induced by SARS-CoV-2 spike protein.



Revealing the secrets to longer-living concrete.



Exploring the protein folding chaperones at the heart of our cells.



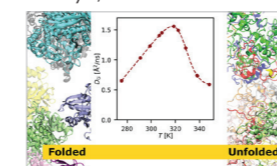
Investigating the batteries of tomorrow.

or read the most recent publications:

<https://www.ill.eu/about-the-ill/documentation/scientific-publications>

ACS Central Science

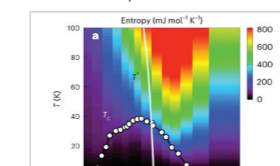
January 9, 2023



Diffusive dynamics of bacterial proteome as a proxy of cell death.

Nature Physics

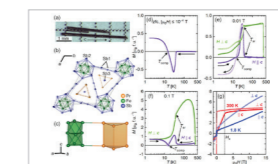
November 17, 2022



Spin fluctuations associated with the collapse of the pseudogap in a cuprate superconductor.

Advanced Materials

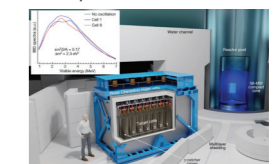
November 30, 2022



Unconventional spin state driven spontaneous magnetisation in a praseodymium iron antimonide.

Nature

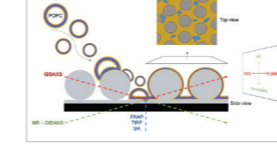
January 11, 2023



STEREO neutrino spectrum of ^{235}U fission rejects sterile neutrino hypothesis.

ACS Applied Materials & Interfaces

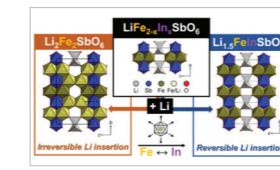
January 10, 2023



Structural characterisation of nanoparticle-supported lipid bilayer arrays by grazing incidence X-ray and neutron scattering.

Chemistry of Materials

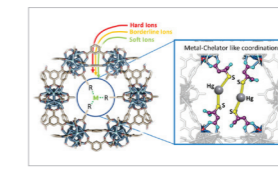
December 23, 2022



Suppression of FE-cation migration by indium substitution in $\text{LiFe}_{2-x}\text{In}_x\text{SbO}_6$ cathode materials.

Chemistry of Materials

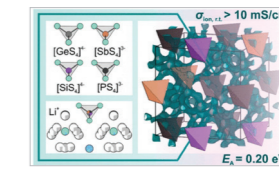
October 24, 2022



Designing metal-chelator-like traps by encoding amino acids in zirconium-based metal-organic frameworks.

ACS Materials Letters

October 6, 2022



A high-entropy multicationic substituted lithium argyrodite superionic solid electrolyte.

Introducing the ILL's Science Colleges

COLLEGE 1 – APPLIED MATERIALS SCIENCE, INSTRUMENTATION AND TECHNIQUES

L. Helfen (*College 1 secretary*)

College 1 deals with research in applied physics and materials science, encompassing industry-related topics as well as new instrumentation and methods in neutron scattering (including scientific computing). Consequently, we receive proposals from a very diverse user community—one that covers metallurgy to cultural heritage—looking to take advantage of techniques such as applied neutron scattering and neutron imaging.

Although all the ILL instruments are accessible via College 1, most of our proposals request beamtime on the imaging instrument **NeXT** and the strain scanner **SALSA**. Additive manufacturing also continues to play an important role, and beamtime at NeXT has often been requested for energy-related and geomaterials research. NeXT is now a fully renovated instrument for state-of-the-art neutron imaging with advanced contrast options, providing intense neutron flux and high spatial resolutions. Measurements here can be combined with X-ray imaging using a microfocus source and can accommodate complex sample environments for *in situ* imaging.

COLLEGE 2 – THEORY

T. Morozova (*College 2 secretary*)

College 2 is dedicated to theoretical modelling in the fields of electronic structure, magnetism and soft matter. It pursues its own research paths and enjoys fruitful collaborations with theoreticians and experimentalists both inside and outside the Institute.

This year several important events took place in the Theory group, with members of the college participating in international scientific events and collaborations. For instance, senior members of the college have established a three-year international research programme that will bring together scientists from Japan (JAEA, Riken) and France (ILL, CEA) working in the field of magnon–phonon couplings. In 2022 the college, together with the Scientific Computing group, organised a simulation day where scientists presented and exchanged computational skills. Lastly, a farewell tribute was held for

two eminent physicists and members of the college, Philippe Nozières and Jacques Villain, both of whom died this year. Their life's work contributed enormously to the scientific life of the ILL, and their influence will continue to be felt for many years to come.

COLLEGE 3 – NUCLEAR AND PARTICLE PHYSICS

C. Michelagnoli (*College 3 secretary*)

College 3 deals with fundamental science, and in particular with nuclear and particle physics. The last shutdown period was used to work on **SuperSUN**, for which a temperature for the converter volume of less than 0.6 K was successfully demonstrated. Work on moving the **FIPPS** instrument to the **H24** end point also started, as has construction of a plunger for fission fragments now that this project plan has been finalised. In addition, preparations for installing Ricochet are now underway.

In 2022, a series of measurements of neutron-capture cross sections important for nuclear astrophysics was successfully performed at the n_TOF facility at CERN. This exercise made use of unique samples of Se-79, Nb-94 and Gd-160 previously produced by high-flux irradiations at the ILL (V4). Additionally, the PF2 team took the opportunity presented by the need to dismantle the pool-side part of PF2's neutron guide system, as part of work on the H1/H2 exchange, to realign and clean the guides. Finally, the VCN beamline benefitted from a major upgrade of the VCN guide and the optical devices, as well as from the introduction of NOMAD as the instrument control system.

COLLEGE 4 – MAGNETIC EXCITATIONS

U. Bengaard Hansen (*College 4 secretary*)

College 4 is dedicated to the study of magnetic excitations. Our main areas of focus are superconductors, ordered and disordered magnetic materials, and frustrated systems. In recent proposal rounds we have seen particularly strong interest in topological materials.

Our proposals are usually well distributed over all the spectrometers designed for magnetic excitations, both time-of-flight spectrometers and the three-axis instruments

at the ILL. Recently, we have seen a significant increase in interest in high-resolution studies using the backscattering spectrometer **IN16B**. Inelastic experiments on magnetic excitation will take advantage of the upgrades on **PANTHER** (five new background choppers) and **IN20** (new graphite monochromator and analyser), as well as the new projects **IN5+** and **D007**—these instruments will provide outstanding performance in terms not only of flux and resolution but also polarisation analysis over the full spectral range.

COLLEGE 5A – CRYSTALLOGRAPHY

O. Fabelo (*College 5A secretary*)

College 5A focuses on crystallographic studies to investigate the relationships between material structure and properties. These investigations are conducted on single-crystal and powder samples, primarily using diffraction instruments. Neutron diffraction is a powerful tool for accurately refining crystalline structures and is frequently used in conjunction with other types of radiation to obtain complementary information.

The College 5A user community comprises seasoned scientists from chemistry and solid- and condensed-matter physics working in a wide range of materials science. These include perovskites, zeolites, organic/inorganic hybrid materials, minerals, inorganic materials and pure organic compounds. More recently, there has been increased interest in more applied studies, including research on gas-storage materials, solar cell materials, ionic conductor materials and *in situ* and/or *in operando* measurements on battery materials.

Users of College 5A will benefit from an increase in flux as a result of the new neutron guides. The most important of these is H24, which will provide light for instruments such as **XtremeD** and **D10+**, both of which are part of the Endurance project. These new instrument capabilities will allow us to make progress in the study of new materials away from non-ambient conditions, in pressure, magnetic fields and temperature. With access to samples of very small diffraction volumes, such as thin film materials, and with the new upgrades, we will be able to push the limits of the type of experiments that can be performed in College 5A.

COLLEGE 5B – MAGNETIC STRUCTURES

J.A. Rodríguez-Velamazán (*College 5B Secretary*) and N.-J. Steinke (*focus group Secretary*)

College 5B deals with the magnetic structures of a broad range of materials investigated using powder or single-crystal diffraction, small-angle neutron scattering and reflectometry. Often polarised neutron techniques are used to study frustrated magnetism and quantum spin liquids, subjects that are of significant interest to our users. Other important subjects in this college include molecular magnets, thin films and the use of very intense pulsed magnetic fields, as well as functional materials such as multiferroics, magnetocaloric compounds and materials for spintronics. In addition, interest in magnetic nanoparticles for biomedical applications, superconductors and skyrmion physics continues to be high. Newer areas of focus include topological materials or new order parameters.

New trends include a move towards skyrmion investigations in thin films that are more oriented towards applications, as well as increasing requests for very demanding experiments that make full use of the capabilities the instruments provide in flux, resolution, polarisation and sample environment. The advent of new instrument projects such as **XtremeD** and **D10+** will offer exceptional capabilities in these areas in terms of flux, resolution, flexibility and sample environment, enabling highly innovative experiments to be performed.

COLLEGE 6 – STRUCTURE AND DYNAMICS OF DISORDERED SYSTEMS

M. Appel (*College 6 secretary*)

The focus of College 6 is disordered systems. While glassy behaviour in polymers and the study of monatomic liquids and gases were previously fields of stronger interest, we are now seeing a trend towards glasses and the domain of confined and porous systems. This change has been accompanied by a steep rise in proposals concerning energy and battery materials, which made up about half of all requests in 2022.

Proposed experiments this year have sought to exploit diffraction from small angles to high Q, including pair distribution function (PDF) analysis (D22/D33, D16, D20, D3 and especially D4) and spectroscopy from sub-picoseconds to hundreds of nano-seconds (**PANTHER**, **IN5**, **IN16B**, **WASP**, and **IN15**). Several of these instruments have undergone substantial upgrades that will increase overall count rates and further improve the level of background, rendering many experiments more efficient and better able to tackle the challenges faced in College 6.

COLLEGE 7 – SPECTROSCOPY IN SOLID-STATE PHYSICS & CHEMISTRY

J. Ollivier (*College 7 secretary*)

College 7 deals with non-magnetic inelastic spectroscopy, bringing together a broad set of scientific fields seeking to use the ILL's inelastic three-axis and spin-echo spectrometers. Phonon studies of the coupling between charges, magnetic moments and lattice degrees of freedom, such as in the magnetocaloric effect, are well represented, as are studies of thermoelectric materials with potential applications ranging from energy-harvesting devices to sensor technology. Light-sensitive materials for electricity production or metrological sensor applications have been a focus in recent years too, not only with the organometallic halide perovskites but also through photosensitive polymers. Clean and energy-saving catalytic chemistry is also under scrutiny. It takes place either through studies of gas diffusion in porous materials with an increased functionalised specific reaction area for gaseous-phase catalysis, or by testing the efficiency of cheap, environmental-friendly substitutes for platinum catalysts such as for hydrogen production.

Overall, the subjects covered by the college show a marked leaning towards Grand Societal Challenges and will greatly benefit from the increased range in frequency and momentum in instruments such as **IN5+**, **PANTHER**, **SHARP** and **WASP**.

COLLEGE 8 – STRUCTURE AND DYNAMICS OF BIOLOGICAL SYSTEMS

O. Matsarskaia (*College 8 secretary*)

College 8 deals with crystallographic, solution and surface studies on biological systems. The diffractometers D19 and LADI exploit the unique capability of neutron crystallography to locate hydrogen atoms. Thus, they provide important structural insights, for example into pathogen–host interactions and drug mechanisms. The arrival of **DALI**, which has higher protein crystallography capacity and a higher resolution mode, will undoubtedly have a big impact in this area.

Structural and thermodynamic parameters of biomolecules in solution can be determined using small-angle scattering (SANS) on D11, D22 and D33; while the interactions of biomolecules with interfaces such as lipid bilayers are studied on the reflectometers **FIGARO** and D17 and on the diffractometer D16. The latter is of particular interest for studies of lipid-based drug delivery and vaccines. The replacement of the **D11**, **D22** and **D16 detectors** with larger and high

count-rate ones will further improve the performance of these instruments. From the spectrometers **IN15**, **IN13** and **IN11**, we can obtain insights into the molecular motions of biological systems including, for example, global and local diffusive dynamics of proteins. Gains in intensity are expected on **IN13+**, primarily due to the performance of the new H24 guide coupled with a new temperature-gradient monochromator.

Last but not least, a large variety of complementary laboratory techniques are available through the EMBL, the PSB platform and the PSCM. Notably, the deuteration of samples, which is crucial for contrast variation experiments, can be performed in collaboration with the ILL's Deuteration Laboratory.

COLLEGE 9 – STRUCTURE AND DYNAMICS OF SOFT CONDENSED MATTER

O. Czakkel (*College 9 secretary*) and S. Micciulla (*focus group secretary*)

College 9 covers diverse topics, often at the interface of physics, chemistry and biology, and every year usually receives one of the highest number of proposals of all the colleges. Recent trends show that these proposed experiments are becoming more and more complex, combining several techniques including *in situ* characterisations such as rheology, dynamic light scattering (DLS) or even small-angle X-ray scattering (SAXS).

Many scientific fields will benefit from the many instrument upgrades undertaken as part of the Endurance programme. **D22** is now equipped with an automatic injection of low viscous samples. From 2024, **D11** users will benefit from its increased flux which will boost contrast variation studies among other things. New modes of operation are now possible on **FIGARO** with its white, un-chopped neutron beam, allowing for sub-second time resolution for kinetic processes or ultra-low surface excess determination of Langmuir and Gibbs monolayers. The two spin-echo instruments, **IN15** and **WASP**, have lower background due to improved Fresnel coils, while additional sample environment equipment developed within the **NESSE** project will enable innovative experiments in many areas. Finally, and importantly, the **chemistry** and **PSCM laboratories** continue to provide full support to our users, who very often need to prepare their samples just before their experiment.

Combined Arrhenius—Merz law describing domain relaxation in type-II multiferroics

Controlling ferroic order, such as ferromagnetism or ferroelectricity, is part of our daily life and promises future technologies in data storage and processing. In a multiferroic material magnetic and ferroelectric order coexist, leading to a strong coupling and to the unique opportunity to drive magnetic order through an electric field. In a type-II multiferroic, a complex magnetic order directly drives the ferroelectric polarisation yielding the tightest connection. While the switching and relaxation of ferromagnetic and ferroelectric domains has been intensively studied using various methods, little is known about antiferromagnetic domain relaxation simply because there is no corresponding external field available. Multiferroics thus open up new opportunities for studying the dynamics of antiferromagnetic domains.

We studied multiferroic domain relaxation in the prototype multiferroic material TbMnO_3 using a stroboscopic technique. The magnetic order in the multiferroic phase of TbMnO_3 is a chiral cycloid, with the two chiral senses corresponding to the up and down direction of the ferroelectric polarisation (along the orthorhombic c direction). In **figure 1**, we show the mounting of a single crystal between two Al plates connected to a high-voltage source. During the measurement this mounting is situated in an Al container, allowing us to control the atmosphere at the sample from outside the cryostat. We can apply either ± 10 kV with moderately low switching times or ± 4 kV with switching times below $50 \mu\text{s}$. We stroboscopically apply the electric field as a rectangular profile alternating positive and negative voltages, and neutrons are counted over many switching cycles.

Experiments were performed on the IN 12 spectrometer using polarisation analysis. By comparing the intensities in the two spin-flip channels for neutron polarisation aligned along the scattering vector, we can directly obtain the domain ratio through the chiral ratio $r_{\text{chir}} = \frac{I_{\uparrow} - I_{\downarrow}}{I_{\uparrow} + I_{\downarrow}}$. The fastest relaxation times that can be analysed with this method correspond to $\sim 50 \mu\text{s}$, while the slowest relaxations are limited by the beam time (~ 5000 s for a half period). In total, multiferroic relaxation processes can be studied over more than eight decades in time.

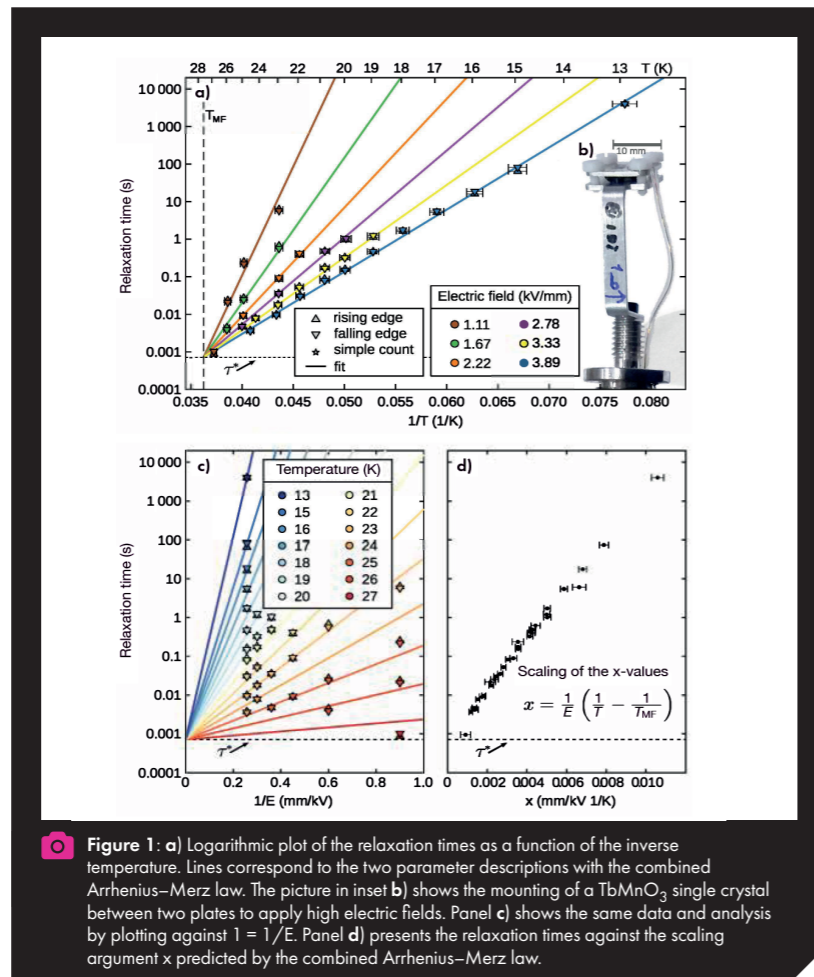


Figure 1: a) Logarithmic plot of the relaxation times as a function of the inverse temperature. Lines correspond to the two parameter descriptions with the combined Arrhenius–Merz law. The picture in inset b) shows the mounting of a TbMnO_3 single crystal between two plates to apply high electric fields. Panel c) shows the same data and analysis by plotting against $1/E$. Panel d) presents the relaxation times against the scaling argument x predicted by the combined Arrhenius–Merz law.

The temperature- and electric field-dependent relaxation times were determined by fitting an exponential relaxation for the two switching directions. We first observe that the relaxation times exhibit an activated behaviour for any fixed value of the electric fields. In addition, these activation laws all coincide when extrapolated to the multiferroic transition temperature $\tau(E, T_{\text{mf}}) = \tau^*$, (**figure 1a**). These two findings yield a rather simple law for the temperature- and field dependence of the multiferroic relaxation: $\tau(E, T) = \tau^* e^{\frac{E}{E_0} \left(\frac{1}{T} - \frac{1}{T_{\text{mf}}} \right)}$. Just two parameters suffice to describe the full temperature- and field dependence over nearly six decades in time (**figures 1a** and **1c**), and the resulting scaling relation is well respected (see **panel d**). The relation corresponds to a combination of Arrhenius activation and the Merz law typically found in ferroelectrics.

It may be surprising that the multiferroic relaxation can be described by quite a simple law, because different processes are involved. The entire relaxation must be dominated by domain-wall motion,

and only close to the multiferroic transition does the inversion of multiferroic domains become faster. The same relaxation law has also been observed in other type-II multiferroics.

In conclusion, we used polarised neutron diffraction with a stroboscopic method to study the inversion of multiferroic domains. The multiferroic relaxation times follow a simple combination of the Merz law and Arrhenius activation that describes the multiferroic relaxation over nearly six decades in time with only two parameters. This relation is also applicable to other type-II multiferroics.

Original publication: Phys. Rev. Lett. (2021) – [10.1103/PhysRevLett.127.097601](https://doi.org/10.1103/PhysRevLett.127.097601)

Contact author: Markus Braden, University of Koeln, Germany. braden@ph2.uni-koeln.de

ILL contact: Karin Schmalzl. schmalzl@ill.fr

Instrument: Three-axis spectrometer with polarisation analysis IN 12

Spin liquid with Ising-like correlations

A spin liquid is an intriguing magnetic state of matter that remains disordered down to zero temperature, yet its constituents—spins—are strongly correlated. A macroscopically degenerate state of this kind was predicted by G.H. Wannier for a triangular antiferromagnet with Ising interactions, as far back as 1950. Our recent experiments, which include diffuse magnetic neutron scattering experiments at the ILL, are the first to realise a spin liquid with predominantly Ising correlations in the triangular spin-lattice compound neodymium heptatantalate.

The concept of a quantum spin liquid (QSL) has, in recent years, become central to the realm of quantum materials. As an emergent, many-body quantum phenomenon, QSL stands alongside other non-trivial states such as those found in superconductors, graphene, topological insulators, Weyl semi-metals, spin ices, etc. Moreover, because it can form stable topologies, the QSL state is also in the spotlight as a potential platform for high-end quantum technologies, e.g. fault-tolerant quantum computations.

This fascinating magnetic state of matter that is highly quantum-entangled but remains magnetically disordered, has in recent years been experimentally observed in various geometrically frustrated materials including realisations of the two-dimensional triangular spin lattice. However, the properties of the recently discovered QSL state in a new triangular lattice antiferromagnet neodymium heptatantalate, $\text{NdTa}_7\text{O}_{19}$, make it the first of its kind—a fluctuating spin liquid with dominant Ising antiferromagnetic nearest-neighbour spin correlations (**figure 1**).

First, we employed inelastic neutron scattering to characterise crystal electric field excitations. This revealed that at temperatures below 10 K the compound behaved as though composed of spin-1/2 degrees of freedom and having extremely strong magnetic anisotropy. In the next step, we used neutron diffraction and muon spectroscopy to show that there was no magnetic ordering even at temperatures of only a few tens of millikelvins, far below the energy scale of the dominant exchange interaction in this compound. Most importantly, neutron scattering experiments performed with polarised neutrons on the D7 instrument at the ILL clearly showed the presence of strong nearest-neighbour

spin-spin correlations at 50 mK but not at 5 K (**figure 2**). These correlations revealed Ising-like short-range ordering, with spins pointing in the direction perpendicular to the triangular planes. Finally, persistently fluctuating local magnetic fields were detected in the ground state via muon spin relaxation, suggesting that quantum fluctuations are crucial for understanding the spin-liquid state of $\text{NdTa}_7\text{O}_{19}$.

The discovery of a QSL with dominant Ising character on the triangular lattice represents a leap forward, in that it confirms the theoretical predictions of an Ising spin liquid made by the Swiss physicist Gregory Hugh Wannier more than seventy years ago. However, additional quantum fluctuations are a salient feature of our discovery, probably emerging from small perpendicular exchange in addition to the dominant Ising exchange, something not seen in any other known material. Our discovery thus introduces a new type of this enigmatic, quantum-entangled state of matter.

The properties of this new QSL can be traced back to large magnetic anisotropy, which is rather typical for rare-earth ions. As the magnetic anisotropy is ion-specific, it is intriguing to imagine various other exotic magnetic states and excitations that could emerge from the broad family of isostructural rare-earth heptatantalate in the future, e.g. as was the case for pyrochlores. In this respect, our study highlights this family of materials as a novel framework for the search for quantum spin liquids and other enigmatic magnetic states.

Original publication: Nat. Mater. (2022) – doi.org/10.1038/s41563-021-01169-y

Contact author: Andrej Zorko, Jožef Stefan Institute, Slovenia. andrej.zorko@ijs.si

ILL contact: Lucile Mangin-Thro. mangin-thro@ill.fr

Instrument: Diffuse scattering spectrometer D7

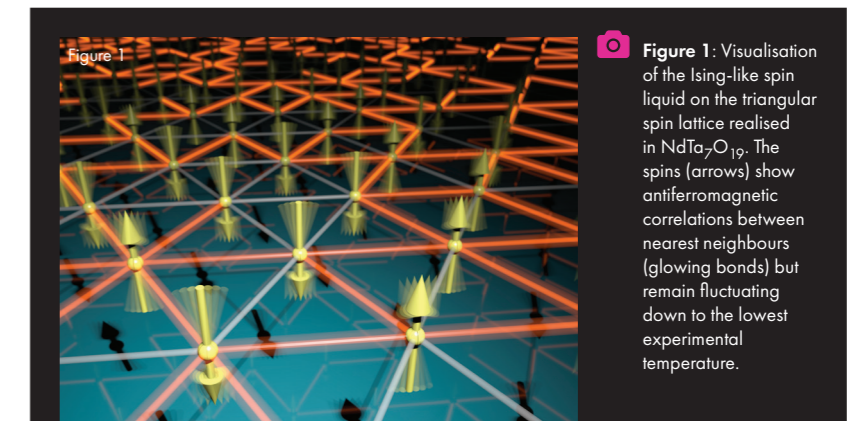


Figure 1: Visualisation of the Ising-like spin liquid on the triangular spin lattice realised in $\text{NdTa}_7\text{O}_{19}$. The spins (arrows) show antiferromagnetic correlations between nearest neighbours (glowing bonds) but remain fluctuating down to the lowest experimental temperature.

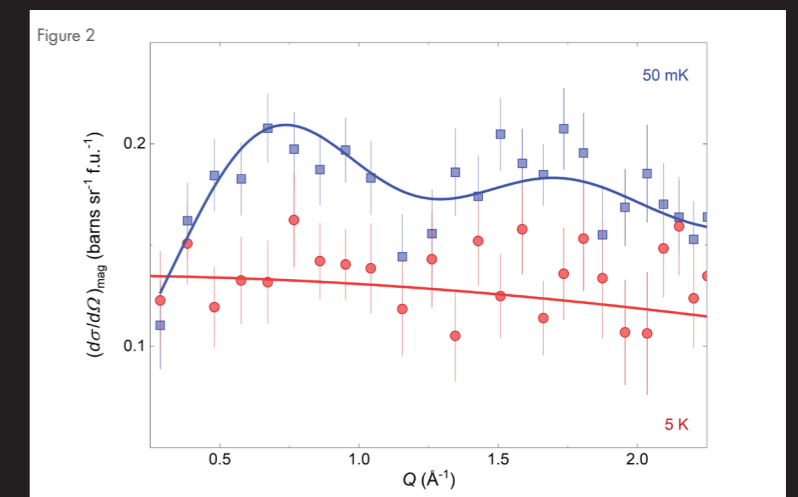


Figure 2: Differential cross section due to diffuse magnetic neutron scattering in $\text{NdTa}_7\text{O}_{19}$ showing paramagnetic response at 5 K (red line) and a clear signature of nearest-neighbour Ising-like correlations at 50 mK (blue line).

Magnetic structure and low-temperature properties of geometrically frustrated SrNd_2O_4

Geometrical frustration combined with antiferromagnetic exchange interactions are key ingredients for the suppression of magnetic ordering down to very low temperatures, but also for complex and fragile ground states sensitive to minute perturbations. In SrNd_2O_4 , the magnetic Nd ions form zigzag ladders consisting of the chains of edge-sharing triangles in a honeycomb-like arrangement. Two distinct crystallographic environments are present for the Nd ions resulting in different crystal electric field levels, another important ingredient for the stabilisation of exotic structures. In this study we combine (un)polarised neutron diffraction and time-of-flight spectroscopy to reveal a partial magnetic order at low temperatures.

The magnetic properties of a family of strontium rare-earth oxides with a general formula ALn_2O_4 ($A = \text{Ba}, \text{Sr}; \text{Ln} = \text{lanthanide}$) have recently attracted considerable attention, as the magnetic Ln ions in these compounds form zigzag ladders with highly frustrated nearest- and next-nearest-neighbour interactions. Further neighbour interactions between different Ln sites link the ladders and form planes of distorted hexagons. Although the strongest interactions are often found within the ladders, the inter-ladder interactions as well as crystal-field effects cannot be ignored.

We investigated a polycrystalline sample of SrNd_2O_4 on various ILL instruments, each adding a piece to the puzzle. The crystal structure was confirmed on the high-resolution diffractometer D2B, while the magnetic ordering was explored on the high-intensity diffractometer D20. The latter revealed the existence of substantial diffuse scattering below 10 K, indicative of short-range magnetic order, which transforms into resolution-limited Bragg peaks at the Néel temperature of 2.3 K. The use of polarised neutrons on the diffuse scattering spectrometer D7 confirmed the magnetic nature of the short-range correlations and their presence even below T_N . From the positions and intensities of the magnetic Bragg peaks in the D20 diffraction patterns, a long-range $\mathbf{q} = (0 \frac{1}{2} \frac{1}{2})$

antiferromagnetic double Néel order was deduced in which the spin sequence along the ladder is up–up–down–down. Rietveld refinement in combination with magnetic symmetry analysis yielded a sizeable ordered magnetic moment for only one of the two Nd^{3+} sites. The magnetic moments on the other Nd^{3+} site have only a small ordered component and remain principally disordered down to the lowest temperatures. Of particular interest is the fact that a predominantly antiferromagnetic inter-ladder exchange is deduced, which differentiates our proposed model from other symmetry-allowed ones (figure 1).

Inelastic neutron scattering measurements performed on the thermal time-of-flight spectrometer Panther show the presence of two well-defined, non-dispersive crystal-field excitations at 5.8 and 15.8 meV (figure 2). The low-lying doublet is responsible for the non-linear temperature dependence of the inverse magnetic susceptibility as well as for the significant magnetic contribution to the specific heat. The excitation seen at 10 meV in figure 2 is due to optical phonons, as concluded from the wave vector and temperature dependence of the scattering.

Our extensive study reveals the particular low-temperature magnetic structure in SrNd_2O_4 as well as the relevant energy scales that will serve to tackle the even more exotic behaviour of this system upon application of an external magnetic field, where heat-capacity measurements suggest a spin-reorientation transition at 30 T.

Original publication: Phys. Rev. B (2021)—
[doi:10.1103/PhysRevB.103.134433](https://doi.org/10.1103/PhysRevB.103.134433)

Contact author and ILL contact: Navid Qureshi. qureshi@ill.fr

Instruments: High-intensity two-axis diffractometer with variable resolution D20, high-resolution two-axis diffractometer D2B, diffuse scattering spectrometer D7, thermal neutron time-of-flight spectrometer PANTHER

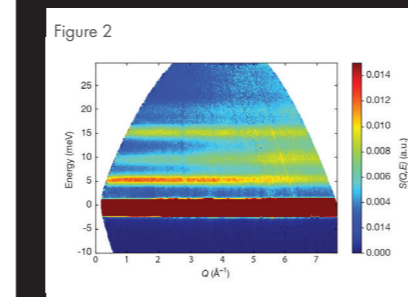
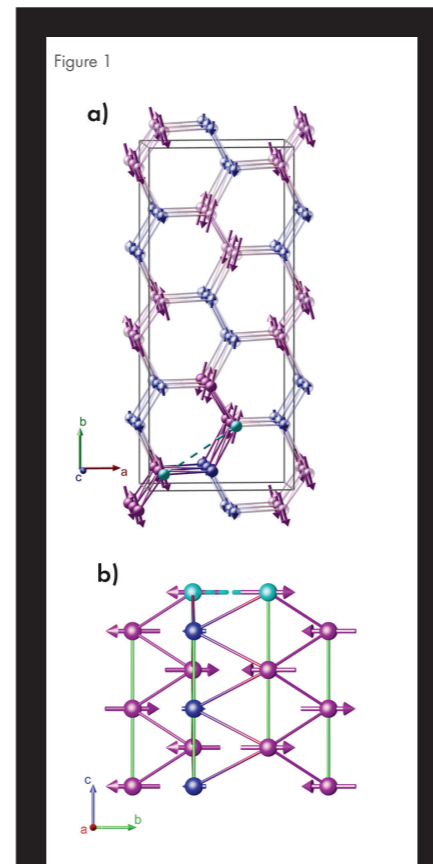


Figure 1: Visualisation of the magnetic structure of SrNd_2O_4 when viewed along the **a)** c -axis and **b)** a -axis. These perspectives allow for a clear visualisation of the antiferromagnetic inter-ladder exchange interactions suspected to induce this ordering scheme.

Figure 2: Inelastic neutron scattering spectra of SrNd_2O_4 at $T = 5$ K measured with an incoming energy of 35 meV.

Deciphering magnetic skyrmion dynamics

A magnetic skyrmion lattice is a topologically non-trivial, vortex-like order of spins, which has been known for some time to form inside a tiny region of the phase space of itinerant-electron helimagnets like manganese silicide (MnSi). In our work, we investigated the magnetic dynamics of a skyrmion lattice in this compound, both experimentally using neutron spectroscopy techniques and theoretically using linear spin-wave theory. We use the theoretical model to quantitatively calculate the ground-state magnetisation, as well as the excitations and their probabilities.

In MnSi , the skyrmion lattice stabilises in a plane perpendicular to an applied external magnetic field, with a tube-like structure forming along the field direction. Very different dispersion relations are observed depending on whether the magnons are excited either along the tubes or inside the two-dimensional skyrmion lattice.

Firstly, along the skyrmion tubes so-called non-reciprocal dynamics are observed, meaning that magnon creation and annihilation do not take place in a symmetric fashion: creation appears at different absolute energies and with different probabilities from those for

annihilation. This is due to the non-centrosymmetric nature of MnSi and the ensuing presence of a Dzyaloshinskii–Moriya interaction between electron spins. The dispersion in this direction is shown theoretically in panel **(a)** of figure 1. The magnon branches comprise a multitude of parabola that are centred around the positions where the magnetic satellite Bragg peaks would be in the adjacent conical phase.

Secondly, inside the two-dimensional skyrmion plane the real-space topology of the skyrmion order forces magnon motion on cyclical paths. Similar to the classical theory of electrons in a magnetic field, the magnon dispersion branches become quantised in closely-spaced Landau bands. For MnSi these bands have an energy difference between one another of about just 10 μeV . They are visualised in panel **(b)** of figure 1, where the Landau levels are shown as thin grey lines and the spectral weights, *i.e.* the probabilities of scattering on certain levels, are indicated by their line thickness. It can be seen that for typical resolutions of neutron spectrometers the close spacing of the bands appears as a quasi-continuous background, while the actual quadratic dispersion relation is created by a modulation of the spectral weights onto these energy levels.

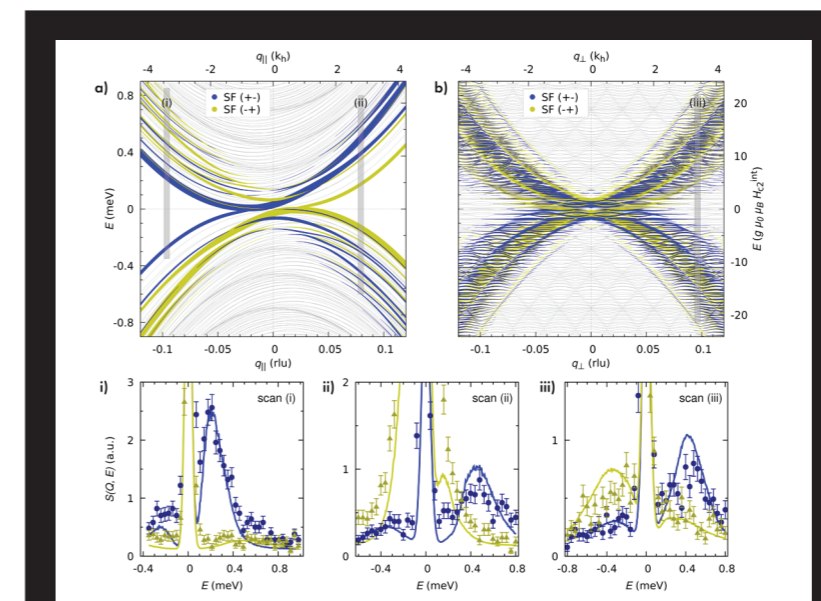


Figure 1: Theoretical dispersion relation for magnons in a skyrmion lattice depicted for **a)** reduced momentum transfers q along the skyrmion tubes, and **b)** inside the skyrmion plane. **i–iii):** Polarised energy scans performed on ThALES (points), as well as resolution-convoluted theoretical curves (lines). For clarity, we only consider transverse fluctuations here. The scans correspond to the positions indicated as grey vertical bars in panels **a)** and **b)**.



ThALES – Three-axis instrument for low energy spectrometry.

Our main series of measurements, which we performed on ThALES, shows very good agreement between the resolution-convoluted theory and the experimental data. This is plotted in panels **(i)–(iii)** of figure 1, where the lines depict the theory. The positions of the measurements correspond to the grey vertical bars in panels **(a)** and **(b)**. We used linear polarisation analysis to partially disentangle the complicated branches and to filter out nuclear scattering contaminating the signal. The blue and yellow colours represent the two spin-flip channels. While it was not possible to individually resolve the finely spaced bands using the three-axis spectrometer, we achieved a very good match between the resolution-convoluted theory and the experimental data.

Our results confirm that the formation of magnonic Landau levels in a two-dimensional skyrmion lattice takes place analogously to the mechanism observed in charge-based systems, being instead based on the electron spin. These results may be important for the development of future low-power spintronic devices, such as racetrack memories or logic gates, featuring magnetic skyrmions as information carriers.

Original publication: Science (2022)—
[doi:10.1126/science.abe4441](https://doi.org/10.1126/science.abe4441)

Contact author and ILL contact: Tobias Weber. tweber@ill.fr

Instrument: Cold-neutron three-axis spectrometer ThALES

The scale of a Martian hydrothermal system explored using combined neutron and X-ray tomography

Water is an essential ingredient for life as we know it, and is central in the search for life elsewhere in the solar system. Ancient riverbeds and deltas in the Martian landscape bear witness to a past when Mars had liquid water on its surface. Furthermore, the occurrence of aqueously altered minerals, as first discovered by the Viking 1 lander in the 1970s, reveals that the rocks reacted with hydrous fluids many times in the geological history of Mars.

Until drill core samples are brought back from Mars, in the early to mid-2030s, scientists wanting to investigate these minerals in laboratories here on Earth are limited to studying Martian meteorites. Nakhilites are a specific type of Martian meteorites that were blasted off the Martian surface by an asteroid impact about 11 million years ago. They are of particular interest as they may shed light on Mars's ancient hydrothermal systems, where once hot water circulated through the bedrock. Such sites are an intriguing target, since hydrothermal systems on Earth can host microbes.

The specimen in this study, MIL 03346, contains clay minerals that crosscut the

mineral olivine. The aqueous alteration took place around 600 million years ago, at a time when liquid water on Mars should have been long gone. To shed light on the origin and timing of the fluids, the researchers used neutron and X-ray tomography, together with scanning electron microscopy (SEM) techniques, to capture the 3D distribution of the hydrous phases. Neutron tomography was chosen because of the neutron's high sensitivity to hydrogen. It was performed on the NeXT instrument at the ILL with a high spatial resolution (pixel size of 7.15 μm). For complementary information about the morphology of other phases in the sample, X-ray tomography scans were performed with an approximately matching effective pixel size of 9 μm , at the 4D imaging laboratory at Lund University. The 3D images were then used as a guide for cutting a slice of the specimen for detailed analysis using SEM, and to validate the segmentation.

The results show hydrous phases clustered both within and around the olivine grains, with limited interconnectivity between the clusters (figure 1). This pattern

suggests that the water responsible for altering these minerals did not leak into the rock from a large-scale hydrothermal system but probably came instead from ice buried within the rock itself that melted due to a meteorite impact. This would suggest that conditions at the particular area where the specimen originated from were not conducive (over a sufficiently long time) to the emergence or development of life.

In conclusion, the use of non-destructive neutron and X-ray tomography is likely to be essential for studying samples brought back from Mars. This study highlights the potential of using neutrons in the search for water in extraterrestrial samples.

Original publication:
doi.org/10.1126/sciadv.abn3044

Contact author: Josefin Martell,
Lund University, Sweden.
josefin.martell@geol.lu.se

ILL contacts: Lukas Helfen. helfen@ill.fr
and Alessandro Tengattini. tengattini@ill.fr

Instrument: Neutron and X-ray
Tomography instrument NeXT

The missing piece: the structure of the $\text{Ti}_3\text{C}_2\text{T}_x$ MXene and its behaviour as a negative electrode in sodium-ion batteries

MXenes constitute a family of 2D materials characterised by some unique structural and functional features. They first appeared in 2011, since when their appeal has continued to increase as an exceptionally broad range of applications for them—such as catalysis, wastewater treatment, cancer therapy, sensors and electrochemical devices—are found. The latter field is emerging as their dominant application, as MXenes possess all the requirements favourable to making them good candidates for fabricating electrodes for rechargeable batteries and supercapacitors.

MXenes are mainly produced from the acid etching of their precursor compounds, the MAX phases of general formula $\text{M}_{n+1}\text{AX}_n$ where M is the transition metal, A is an element from group 13 or 14 and X is C and/or N. This procedure involves the withdrawal of the A element leading to the formation of the MXene structure (general formula $\text{M}_{n+1}\text{X}_n\text{T}_x$ with T the new functional termination group replacing the A element). Of the various compositions, Ti_3AlC_2 is the most common MAX phase, the derived MXene compound having the general formula $\text{Ti}_3\text{C}_2\text{T}_x$ where T = F, O, OH (figure 1).

The combination of the synthesis procedure and the peculiar structure of the MAX phase generates the conditions for obtaining the MXenes as highly disordered crystalline structures. It is generally accepted that even if the structure and composition of the Ti_3C_2

layers of MAX and MXene phases are the same, the etching procedure leads to a completely different electronic structure that strongly affects the electrochemical performance of the material. Indeed, the electrochemical performance directly depends on the nature of the termination group, interlayer distance and degree of crystallinity of the material.

In the present study, we combined different techniques to identify the MXene structure. X-ray absorption measurements provide information about the oxidation state and local environment of the Ti centres, while X-ray photoelectron spectroscopy gives information about the termination's composition (relative F/O ratio). The building blocks for modelling the local structure of the MXene were obtained by combining the results of these two methods with previous theoretical calculations.

The core element of the study was the analysis of the neutron diffraction data collected on the high-resolution powder diffractometer D2B at the ILL. To account for the complexity of the long-range structure we used the Faults software, which is able to describe the structures as sequences of layers and to introduce 2D defects.

Data were acquired for both the precursor MAX phase and the MXene samples. The MAX phase data were analysed using the traditional Rietveld refinement approach in order to validate the approach embodied in the Faults software for

this specific case. The high degree of agreement between the results motivated us to attempt the analysis of the MXene data. The results obtained indicate that the main source of disorder in the MXene samples is the presence of stacking faults.

Our study has led, for the first time, to a satisfactory fitting of diffraction data for MXenes. We were able to identify a quantitative parameter that can discriminate between different MXenes characterised by different degrees of disorder. In fact, MXenes obtained under different experimental conditions exhibit different termination compositions (in terms of F/O ratio) but the same Ti_3C_2 layer structure. In all the MXenes produced the stacking faults are massively present, the main difference being the distribution in the interlayer distance spacing. This is also the origin of the macroscopic differences in morphology and in the functional properties, such as the irreversibility observed in the first cycles of the electrochemical testing and the different specific charge capacity.

Original publication: <https://pubs.acs.org/doi/10.1021/acs.nanolett.1c02809>

Contact author: Chiara Ferrara,
Università degli Studi di Milano-Bicocca,
Italy. chiara.ferrara@unimib.it

ILL contact: Emmanuelle Suard. suard@ill.fr

Instrument: High-resolution two-axis diffractometer D2B

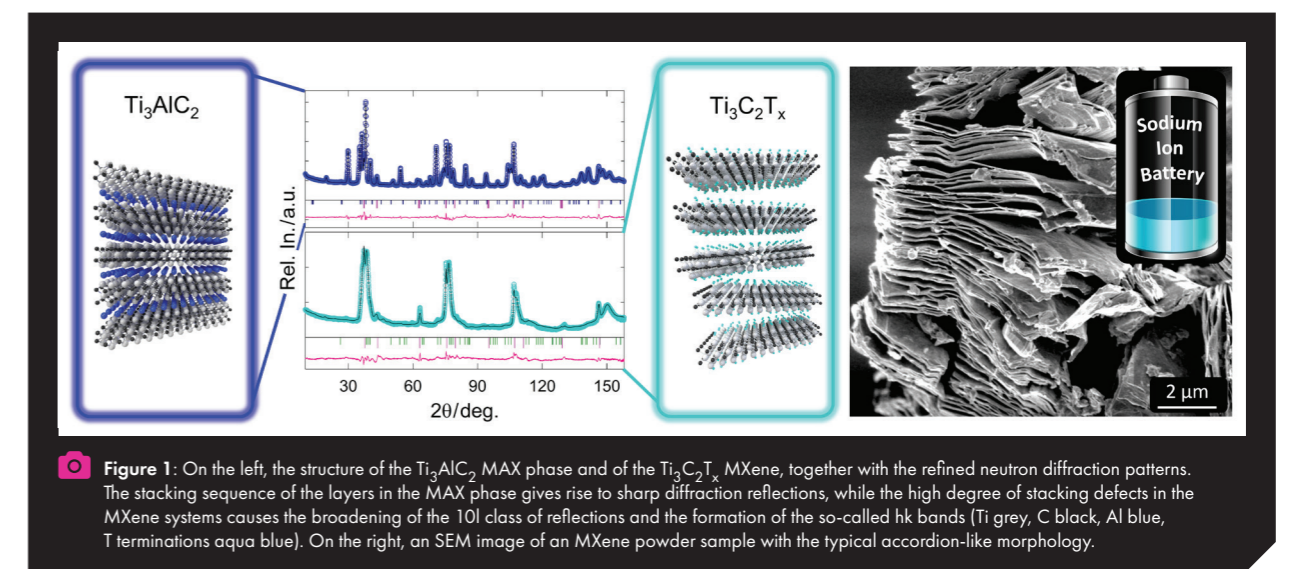
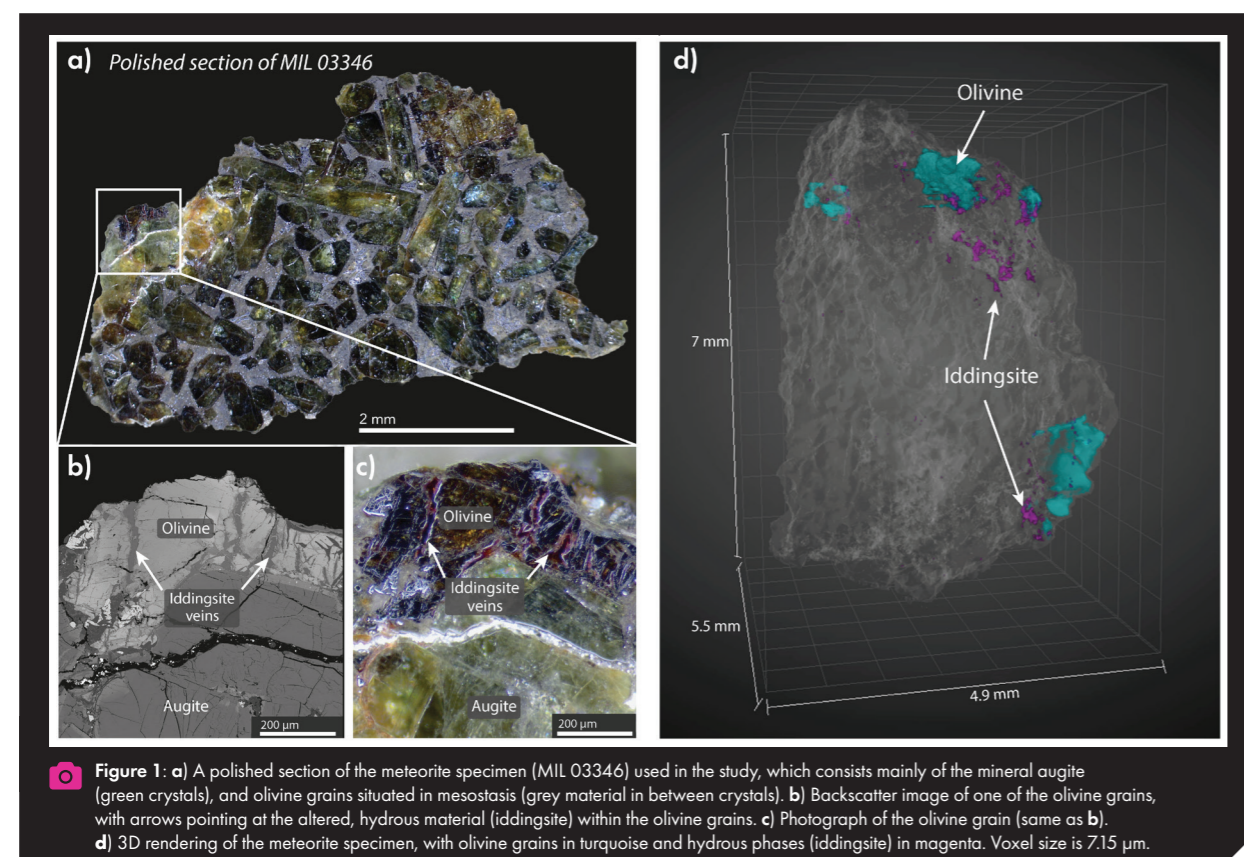


Figure 1: On the left, the structure of the Ti_3AlC_2 MAX phase and of the $\text{Ti}_3\text{C}_2\text{T}_x$ MXene, together with the refined neutron diffraction patterns. The stacking sequence of the layers in the MAX phase gives rise to sharp diffraction reflections, while the high degree of stacking defects in the MXene systems causes the broadening of the 10l class of reflections and the formation of the so-called hk bands (Ti grey, C black, Al blue, T terminations aqua blue). On the right, an SEM image of an MXene powder sample with the typical accordion-like morphology.

Overall structure of the fully assembled cyanobacterial KaiABC circadian clock complex using an integrated experimental–computational approach

The integrity of a biological system is maintained by its homeostatic activities, including the dynamic assembly and disassembly of biomolecules—effectively, its circadian rhythm. In cyanobacterial circadian regulation, three key proteins (KaiA, KaiB and KaiC) assemble to form the KaiABC complex. Cryogenic electron microscopy (cryo-EM) studies can identify most of the structure of this complex, but the KaiA protomers seem to be a bit shy when researchers try to examine them microscopically. In this study we attempted to elucidate the full-length structure of $A_{12}B_6C_6$, including its dynamically fluctuating domains, by combining small-angle neutron and X-ray scattering (SANS, SAXS) with computational methods.

Solution scattering is one of the methods used to perform the structural analysis of biomacromolecules in solution, providing a structure close to the native state and dynamically fluctuating. In this article we describe the structure of a large protein complex possessing dynamical fluctuating domains, using a combination of solution scattering experiments and computational methods.

Cyanobacteria has a circadian clock in which three proteins—KaiA, KaiB and KaiC—alternate dissociation and association phases in the presence of ATP, over a 24-hour cycle. The structure of the largest

complex of the three proteins, the ABC complex, was first reported by Snijder *et al.* using cryo-EM (figure 1a). The complex, consisting of 12 KaiA, 6 KaiB, and 6 KaiC, has a ring structure: the base unit is a cylindrical BC complex (yellow and grey), and 6 KaiA dimers (pink and cyan) surround the KaiB hexameric ring like a crown. While the cryo-EM study revealed the arrangement of the C-terminal domains of the KaiA dimers (C_A), the structure lacks the N-terminal domains of the 6 KaiA dimers (N_A) due to their dynamical fluctuation. In this study we attempted to elucidate the full-length structure of $A_{12}B_6C_6$, including its dynamically fluctuating domains, by combining SANS, SAXS and computational methods.

A SEC (size exclusion chromatography)–SAXS was first applied to obtain the scattering profile of the overall structure of ABC complex in solution (figure 1b, top), *i.e.* including its fluctuating parts. To highlight KaiA's contribution, SEC-iCM (inverse contrast-match)–SANS, a state-of-the-art method, was performed to obtain the scattering profile of KaiA protomers within the ABC complex while matching out KaiB and KaiC contributions. (The complex was prepared using 75 % deuterated KaiB and KaiC and hydrogenated KaiA). The D22 SEC–SANS set-up using a 100 % D_2O buffer for elution enabled us to measure the scattering signal coming only from KaiA protomers within the ABC complex (figure 1b, bottom).

The structural analysis was performed using a combination of computer modelling, SAXS/SANS data and molecular dynamics (MD) simulations. First, starting with the cryo-EM and crystallographic structures, computational modelling was used to explore all possible positions of the KaiA N-terminal domains (N_A). This resulted in 20 million full-length structural models. Second, all the models were compared with the SAXS data and 8 600 were found to provide a reasonable fit. These 8 600 SAXS-filtered models were then classified into three structural groups, depending upon the locations of the N_A domains, and further compared with the iCM–SANS data. A total of 250 models belonging to one structural group were able to explain the SANS curve. Finally, the 250 models were classified into eight sub-groups according to the symmetry of the N-terminal domains of the KaiA protomers, and an MD simulation performed for each sub-group.

One sub-group showing long-term stability was selected as representing the structure of full-length $A_{12}B_6C_6$ complex in solution. As shown in figure 1c, there are two configurations of the N_A domains. The red domains are located between adjacent KaiA C-terminal (C_A) domains (pink and cyan), possibly contributing to the stability of the KaiA ring structure. The blue domains shield the two C_A domains' interface (highlighted by the black and white dashed areas in figures 1a and 1c, respectively), preventing KaiC from destabilising it.

We believe that our approach, using the compelling combination of SAXS, SANS and MD simulations, has accurately determined the structure of the complex with its dynamical fluctuating domains, and offers a signpost for future integrated structural analysis.

Original publication: Commun. Biol. (2022)—doi.org/10.1038/s42003-022-03143-z

Contact author: Hidetoshi Kono, National Institutes for Quantum Science and Technology (QST, Japan). kono.hidetoshi@qst.go.jp

ILL contact: Lionel Porcar. porcar@ill.fr

Instrument: Small-angle scattering diffractometer D22

Neutron crystallography sheds light on the initial stages of *Pseudomonas aeruginosa* infection

Pseudomonas aeruginosa is a human pathogen that causes hospital-acquired infections in immunosuppressed people. The first stages of infection include bacterial colonisation and the formation of a bacterial biofilm. Here, sugar-binding proteins produced by the bacteria play a role as they bind to the host cells. Detailed structural knowledge of these interactions is important for the design of new drugs in the prevention and treatment of bacterial infection.

Antibiotic resistance is one of the major global threats of the 21st century and requires the development of new effective treatments. *Pseudomonas aeruginosa* is an opportunistic human bacterial pathogen and one of the most commonly associated with hospital-acquired infections. Due to its increasing resistance to antibiotics it can also cause fatal infections in immunocompromised or cystic fibrosis patients. *Pseudomonas* bacteria produce many virulence factors, including sugar-binding proteins called lectins which are involved in the initial stages of host infection. One of them, LecB, is specific to L-fucose, a monosaccharide that is present on the surface of host cells in the form of glycosylated proteins

and lipids. Lectins help bacteria to read this complex 'glyocode' by targeting specific carbohydrates during attachment to the host cells.

LecB lectin is viewed as a potential drug target for glycomimetic compounds used in anti-adhesive therapy, which has the advantage over antibiotic therapy of not promoting resistance. LecB is a tetrameric protein that displays an unusually high affinity towards fucose, with a unique binding site containing two calcium ions directly involved in sugar binding. X-ray crystallography produced high-resolution structures of the complex, but questions about protonation states and water orientation remained unanswered.

Neutron macromolecular crystallography (NMX) offers unique insights into ligand binding as it directly locates and allows visualisation of all hydrogen (or deuterium) atoms involved in the interactions. Perdeuteration, where all hydrogen atoms are replaced by deuterium atoms, enhances their visibility in the neutron maps. While perdeuteration of recombinant proteins is carried out almost routinely in dedicated deuteration facilities, the production of perdeuterated sugars is still very challenging.

In collaboration with the Centre de Recherches sur les Macromolécules Végétales (CERMAV, CNRS) Grenoble, we used perdeuteration (carried out in the D-lab facility at the ILL) and NMX to yield a neutron structure of the perdeuterated LecB/fucose complex using the LADI instrument at the ILL. The structure gave us new insights, in unprecedented detail, into the tight binding between the sugar and the protein.

The study enabled a complete description of the hydrogen-bonding network between the sugar and the protein (figure 1). We could observe that all the charged amino-acid residues involved in the calcium co-ordination were non-protonated. Interestingly, we also observed a low-barrier hydrogen bond, a special type of strong hydrogen bond between one of the fucose hydroxyl groups and the protein. Moreover, the orientation of water molecules involved in the interaction could be discerned, revealing higher mobility than had previously been thought based on the X-ray structures.

Neutrons played an important role, as none of these details could be revealed using X-ray crystallography alone. The high affinity of LecB to fucose could be explained by a synergy between the short hydrogen bonds in the binding site that results in unique charge delocalisation, and the dynamic behaviour of bridging water molecules at room temperature. The new structural data may help in the design of potent new glycomimetic compounds for fighting antibiotic-resistant bacteria. They also pave the way for studies of more complex systems, including the natural oligosaccharides present on human cells.

Original publication: Nat. Commun. (2022)—[doi:10.1038/s41467-021-27871-8](https://doi.org/10.1038/s41467-021-27871-8)

Contact author: Lukas Gajdos and Juliette M. Devos, ILL. gajdos@ill.fr

ILL contact: Matthew P. Blakeley. blakeym@ill.fr

Instrument: Quasi-Laue diffractometer LADI and DALI

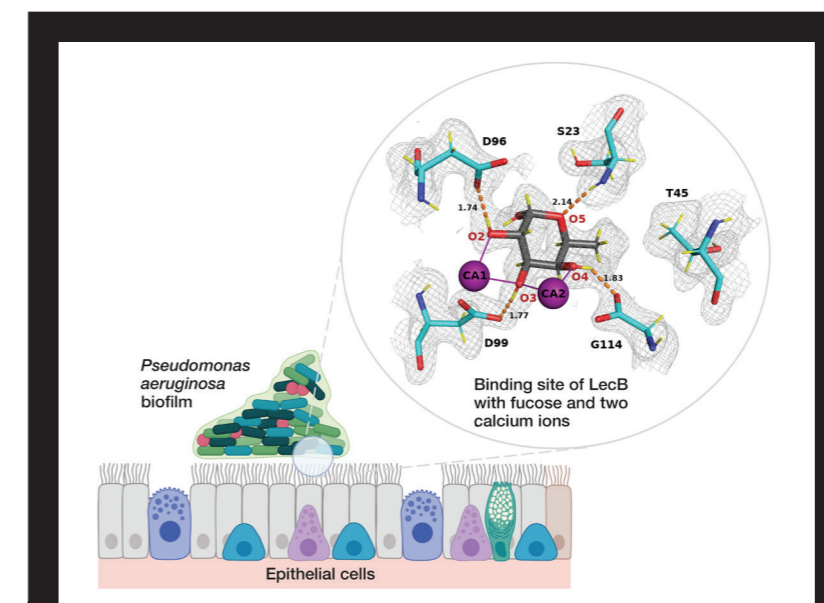


Figure 1: Schematic representation of *Pseudomonas aeruginosa* infection, with a close-up of the fucose-binding site of LecB lectin. Grey mesh represents neutron density, purple spheres represent calcium ions, and black and cyan sticks represent fucose and protein, respectively.

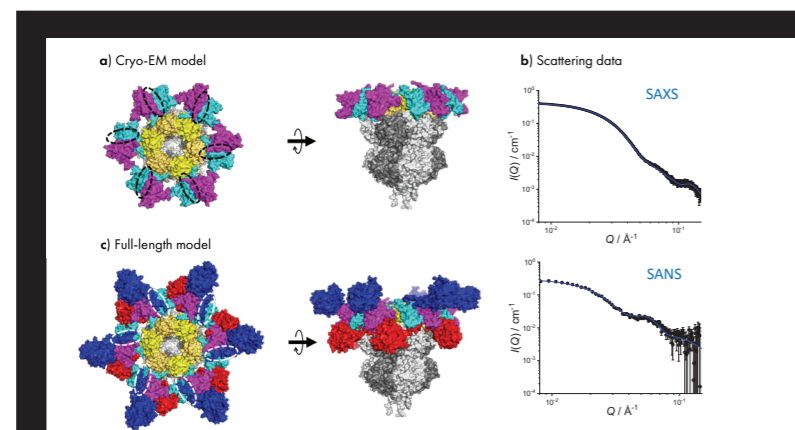


Figure 1: a) Top and side view of the overall structure of the KaiABC complex determined by cryo-EM. The structure is lacking the N-terminal domains of KaiABC. Grey, yellow magenta and cyan denote KaiC, KaiB, and two C-term domains, respectively. b) SEC-SAXS profile of the overall structure of the KaiABC complex in solution (top) and SEC-SANS profile of the KaiA out of the KaiABC complex (bottom). The grey line denotes the averaged profile calculated using the structures obtained by MD simulations. c) The complete, overall structure of KaiABC. The missing N-terminal domains of KaiA in the structure of a) are shown in blue or red.

Probing foams from the nanometre to the centimetre scale

Liquid foams—a dispersion of air in a liquid—exhibit unique characteristics that make them ideal candidates for a variety of applications. For example, the food business appreciates foam for its lightness and unctuousness, while the fire service finds it beneficial for its capacity to fill huge spaces while acting as an insulating barrier. Foam also enables the pharmaceutical and cosmetics industries, among others, to cut costs by reducing the amount of active ingredients they use. Foams are ubiquitous in daily life. However, they are also incredibly fragile since they are physically unstable, and it is still very difficult to estimate how long they will last. In order to track the various factors involved in the ageing of foam it is crucial to characterise it in its totality, from the foam bubble of a few centimetres in size, to the film which might be only few nanometres thick.

The structural characterisation of liquid foams, which are multi-scale systems, necessitates the combination of a wide variety of methodologies. Because foams are inherently unstable systems, this already hard investigation is rendered even more challenging, as the results performed on different instruments are not always straightforward to compare. To tackle the task, a novel apparatus has been developed at the ILL that enables the time-resolved investigation of foams by simultaneously recording small-angle neutron scattering (SANS), electrical conductivity and bubble imaging. Small-angle scattering provides a structural characterisation of the foam films, as well as of particles—such as micelles—present in the foam; electrical conductivity allows us to precisely determine the water amount in the system, while imaging techniques provide a characterisation on the bubble size and its temporal evolution. These technical innovations are combined with a novel formalism to analyse the SANS scattering data in absolute units, allowing us to extract additional valuable information on the foam such as the specific area of the foam film. Using this tool and other analytical techniques, the time-resolved characterisation of foams can be carried out in a single experiment at scales ranging from the nanometre to the centimetre.

Figure 1 shows a classical experimental dataset obtained using this multi-scale set-up, with (a) the photograph of the foam and (b) the corresponding 2D SANS data on the central detector obtained at the end of the experiment for a 73-minute-old foam. The liquid fraction determined from the conductivity (c) and the radially averaged SANS data (d) are plotted as a function of time (last curve in red for the 73-minute-old foam) to emphasise the large variation in the foam's structure during its ageing process.

The device also enables the progress of bubble size to be tracked using macrophotography, as well as providing complete information on the foam film's thickness and Plateau borders through the SANS data. By correlating the thickness of the inter-bubble film and the capillary pressure (determined from image analysis of the Plateau borders' radius), it is possible to monitor the internal pressure within the films prior to their rupture for the first time for a draining foam (as shown in figure 2), with a view to better understanding the coalescence phenomenon.

In summary, analysis of foam stability requires the simultaneous collection of a wide range of information, on scales ranging from the nanometre to the centimetre. Correlating this information can lead to a better understanding of the underlying processes that destabilise foams. Obtaining such a detailed overview of the evolution of foam is a fundamental step towards being able to design novel foams with desired properties. We now aim to use this new set-up to address fundamental physical questions, e.g. on the foam ageing mechanisms and applied problems, for sustainable food systems, and rare earth recovery.

Original publication: Soft Matter [2022]—<https://doi.org/10.1039/D2SM01252A>

Contact author: Julien Lamolinarie and Leonardo Chiappisi.

ILL contact: Leonardo Chiappisi. chiappisi@ill.fr

Instrument: Small-angle scattering diffractometer D33

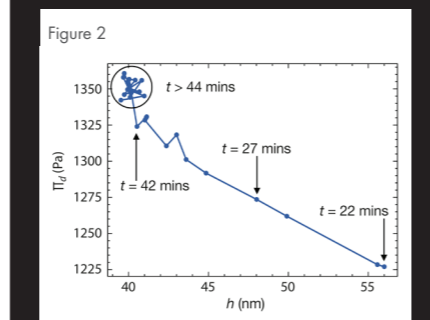
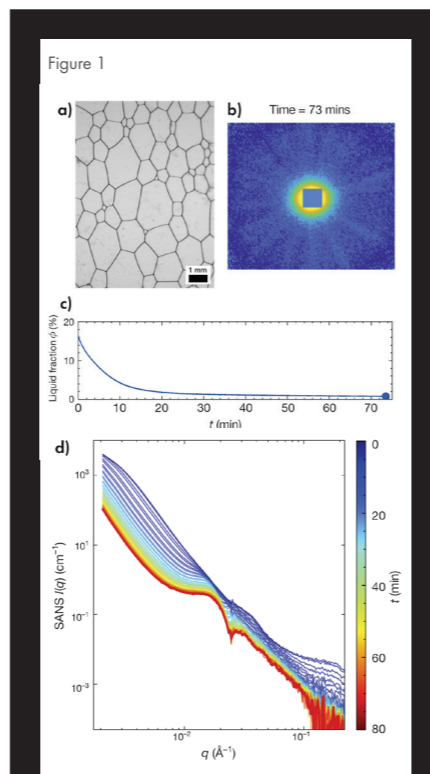


Figure 1: Classic set of experimental data collected at 73 mins, with (a) the photograph of the foam, (b) the 2D SANS data on the central detector, (c) the liquid fraction determined from the conductivity measurements and (d) the radially averaged SANS data as a function of time (in red for the 73-minute-old foam).

Figure 2: Internal pressure in the film calculated from the values of the Plateau borders as a function of film thickness, obtained from SANS data analysis.

Ligand dynamics in nanocrystal solids studied with quasi-elastic neutron scattering

Nanoscience and nanotechnology have opened up new dimensions for society in the past 20–30 years. The relevance of surface and quantum effects has allowed us to create novel materials with tunable and improved properties. Colloidal nanocrystals (NCs) are an important class of nanomaterials for both fundamental research and industry. Their distinguishing feature is the ligand shell around the NCs. The ligand shell greatly determines the size, morphology, stability and structural organisation of the NCs. Looking in more detail, the tethering of ligands on the NC surfaces influences the structure and dynamics of the surface layers (and vice versa), and thereby the macroscopic properties too. Moreover, the ligand shell provides the connectivity between NCs; therefore, all macroscopic transport properties are strongly linked to the nature of the ligand shell.

We used quasi-elastic neutron scattering (QENS) to compare the dynamics of different ligand molecules in lead sulfide (PbS) nanocrystalline solids (figure 1). PbS is one of the most studied examples of colloidal nanocrystals, mainly because of its interesting optoelectronic properties.

From the neutron scattering point of view, PbS is a highly coherent scatterer that makes negligible contribution to the measured spectra compared with the organic ligands in the relevant momentum transfer (Q) range.

Surprisingly, although neutrons can provide unique insights, only very few such experiments have been conducted on related systems. We were able to obtain a comprehensive picture of ligand motions by combining experiments performed on the backscattering spectrometer IN16B at the ILL ($dE = 1 \mu\text{eV}$) with those conducted on the time-of-flight spectrometer FOCUS at the PSI ($dE = 45 \mu\text{eV}$) (figure 2). Furthermore, elastic and inelastic ($@ E = 3 \mu\text{eV}$) fixed window scans were performed. These provide an overview of the thermal activation of different motions and are often also an economical way of determining the corresponding activation energies.

The double-peak-shaped inelastic fixed window scans revealed the existence of two different motions. The two spectrometers captured these two processes for all our samples, and we obtained a good fit for all data with the same parameter set on both instruments. We observed no long-range translational diffusion, thereby confirming

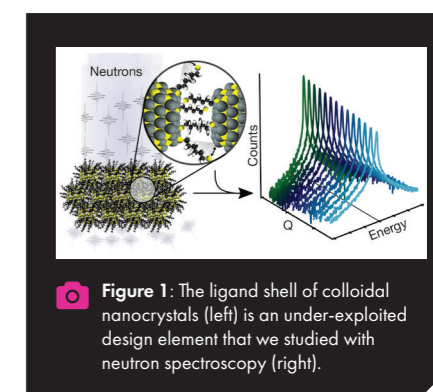


Figure 1: The ligand shell of colloidal nanocrystals (left) is an under-exploited design element that we studied with neutron spectroscopy (right).

that all ligands are bound to the NCs at (and below) 300 K. We assign the faster process to a precession and the slower one to a uniaxial rotation, based on the Elastic Incoherent Structure Factors (EISF) (figure 2). Several models in different combinations were tested, whereby some parameters, such as rotation radii, were fixed in accordance with density functional theory (DFT) simulations. Surprisingly, we could find no clear evidence of a separate activation, nor of the existence of methyl rotation in the case of the monothiol, only a weak indication via the fit parameters. In all cases, a fraction of the ligands was immobile during the observation period.

In summary, we found that the precession of rotating monothiol can be suppressed through simultaneous binding of both ends to neighbouring NCs; or it can be restricted, as a result of the different behaviour of thiol- (-SH) or methyl- (-CH₃) groups. In addition, the symmetry of the backbone is reflected in the geometrical details of the uniaxial rotation. Shorter chains are more active, probably because of less interpenetration and a higher degree of disorder. Finally, but importantly, we observed lower activation energy for shorter chains and for the dithiol samples.

These findings not only have direct relevance to the thermodynamical description of nanocrystalline solids, they are also crucial for upcoming work on the elastic properties of the ligand shell.

Original publication: ACS Nano (2021)—<https://pubs.acs.org/doi/full/10.1021/acsnano.1c09073>

Contact author: Fanni Juranyi, PSI, Switzerland. fanni.juranyi@psi.ch

ILL contact: Tilo Seydel. seydel@ill.eu

Instrument: Backscattering spectrometer IN16B

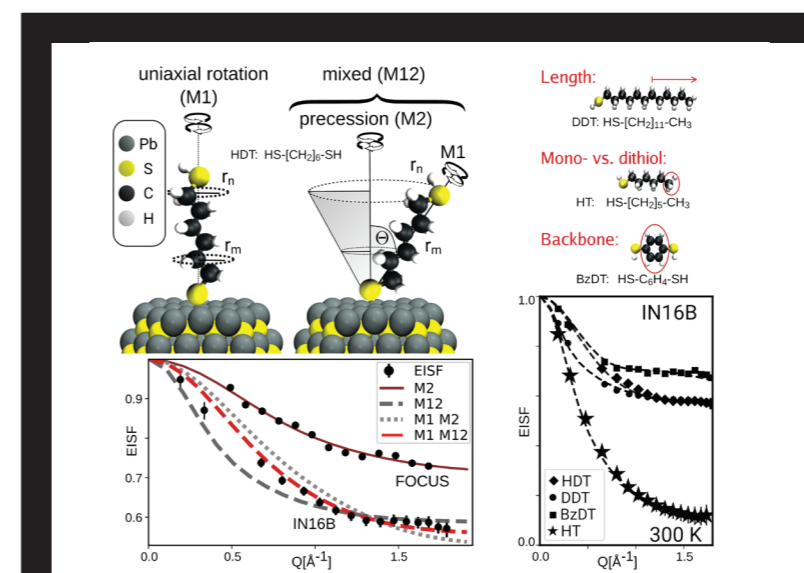


Figure 2: Dynamics of ligand molecules on PbS nanocrystals measured on the backscattering spectrometer IN16B (ILL) and the time-of-flight spectrometer FOCUS (PSI) using quasi-elastic neutron scattering. The geometry of the localised motions was established based on the Elastic Incoherent Structure Factors (EISFs). Left: Illustration of the identified motions of the HDT Ligand. On the FOCUS observation time scale part of the ligands perform a precession motion (M2), whereas IN16B reveals that on longer time scales these ligands also rotate around the molecular axis (M12), together with other ligands, which appear immobile on FOCUS (M1). Right: We also examined the effects of chain length, functionalisation and backbone geometry, where the same types of motion, but with different parameters, were found.

Entangling the dynamics of colloidal networks with macroscopic responses

The development of novel molecular gels based on environmentally friendly components is key to advances in technologies for drug delivery to stimuli-responsive materials. For these systems, understanding their structure–dynamics–function relationship becomes essential for designing new materials with the desired properties. We explored the structure and dynamics of three compositionally identical colloidal systems composed of sugar-based surfactants with very different gelation properties. We show how the dynamic response of the entangled gel network relates to the flexibility of the individual worm-like micelles, which is ultimately connected to the rheology of these ‘noodle soups’.

We investigated the nanoscopic and mesoscopic dynamics of assembled networks composed of sugar-based surfactants. These molecular building blocks have the particular characteristic of being identical in terms of chemical composition but different in the geometry of the molecule. In terms of chemical structure, changing the anomeric configuration of the headgroup and/or the tail unsaturation leads to monomers with different ‘architecture’, i.e. from straight to bent molecules (figure 1). Upon self-assembly, different nanostructures are formed depending on that architecture. Those differences extend to the macroscopic level and induce a different rheological response: bent molecules result in more fluid systems, while the straight molecules form strong viscous gels. So, the question we asked ourselves was this: How can these small differences at the molecular level cause such big differences in behaviour?

We studied these systems using a combination of neutron spin echo (NSE) and 3D cross-correlation dynamic light scattering (DLS). The neutron experiments were performed on IN15, a world-leading NSE instrument with the capacity to access the dynamics of soft materials at the nanoscopic level. From the NSE and DLS data we extracted the characteristic diffusion modes of the nanostructures (figure 2). The results revealed three characteristic dynamic regimes: the structural fluctuations in the individual micelles (aka, flexibility), the breathing dynamics of an individual network and the co-operative diffusion associated with the entanglement between the different networks.

Our results show that the dynamics of these systems are connected to the structure of the assemblies, ultimately controlling the rheology of the system. The bent molecules pack less efficiently, resulting in shorter micelles that freely diffuse without major interference with other micelles. Thus, these systems show low viscosity. The straight molecules show more efficient packing, resulting in very long (noodle-like) structures. These structures form entangled networks with topological constraints, and this results in the formation of strong gels.

These results provide a framework for developing materials with tailored functions from a new perspective. Now, materials such as hydrogels can be designed from a library of geometrically varied molecular building blocks without altering the chemical composition of the system. Importantly, these building blocks can be synthesised from renewable materials, establishing a route within the boundaries of Green Chemistry.

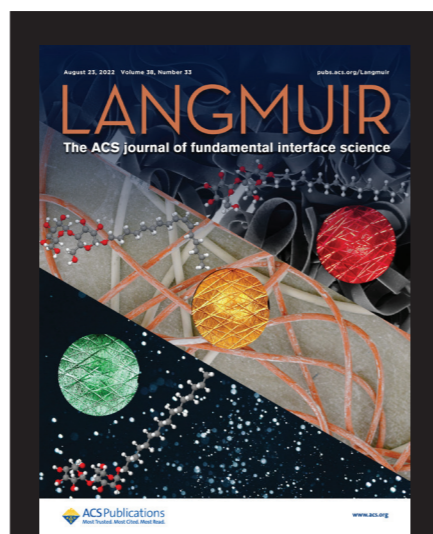


Figure 1: Front cover of the *Langmuir* journal. The cover depicts the three different molecular geometries investigated in the article and the concomitant ‘traffic’ motions: green light = freely diffusing; yellow light = weakly arrested; and red light = strongly arrested.

Original publication: *Langmuir* (2022)—[doi:10.1021/acs.langmuir.2c00230](https://doi.org/10.1021/acs.langmuir.2c00230)

Contact author: Adrian Sanchez-Fernandez, Universidade de Santiago de Compostela, Spain. adriansanchez.fernandez@usc.es

ILL contact: Orsolya Czakkel. czakkelo@ill.fr

Instrument: Spin-echo spectrometer IN15

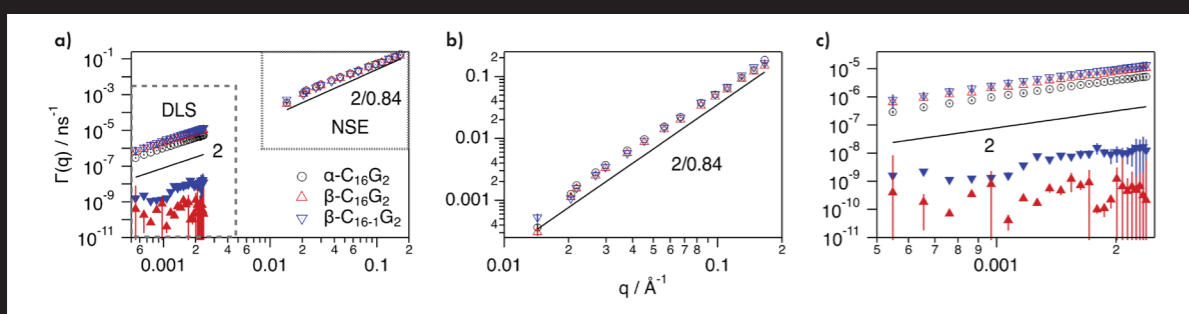


Figure 2: a) Relaxation rates (aka, dynamics) of the assembled structures formed by the three surfactants investigated by b) NSE and c) DLS. Our results show how the characteristic nanoscopic dynamics begin to diverge at the segmental length scale (low q in the NSE data) to result in distinct motions at the mesoscopic level (DLS data).

Unveiling the $S = 3/2$ Kitaev honeycomb spin liquids

The $S = 1/2$ Kitaev honeycomb model (KHM) is a unique, exactly solvable spin model displaying a quantum spin liquid (QSL) ground state that has become a cornerstone of phase studies thanks to its implementations in solid-state. In this work, using a mean-field theory we revealed the phase diagram of the $S = 3/2$ KHM, which displayed extraordinary agreement with state-of-the-art DMRG simulations. These are timely results given recent proposals for implementing higher- S KHMs.

The KHM is the paradigmatic model hosting QSLs characterised by a static Z_2 gauge field coupled with Majorana fermion excitations. Initially proposed as a toy model for studying topological quantum computation, its experimental interest sky-rocketed after it was proved to be relevant in explaining magnetic excitations of $j=1/2$ layered Mott insulators. Novel routes to these so-called Kitaev materials have been investigated over the last four years, opening up the possibility of finding $S = 1$ and $S = 3/2$ KHM platforms. Unfortunately, analytical treatments of this model were successful only for $S = 1/2$ or $S \geq 2$. On the theoretical side, the $S = 3/2$ case has been highlighted because here even

numerical methods seem unreliable, due to a large number of low-energy excitations hindering identification of its ground state. The same model has also become important in the study of magnetic nanodevices since its use on chromium-based magnets that can be exfoliated into graphene-like monolayers was proposed.

Our work showed how a Majorana parton representation of $S = 3/2$ multipole operators maps the $S = 3/2$ KHM onto a free-fermion problem of static gauge fields whose product over closed loops represents conserved Z_2 fluxes. On a fixed sector, the $S = 3/2$ KHM is represented by a non-quadratic Hamiltonian of Majorana fermions with three distinct Majorana flavours. A mean-field theory of this model under a specific single-ion anisotropy allows the system to be analytically tractable and reveals a phase diagram with four distinct QSLs. Three of the QSLs coexist with quadrupole orders, and two of those phases are adiabatically connected to the $S = 1/2$ Kitaev spin liquid. The remaining QSL is gapless and displays two Majorana flat bands that are closely related to a quantum spin-orbital liquid emerging from an exactly solvable model. The mean-field results show quantitative agreement with complementary DMRG simulations.

We hope that our work can provide a useful starting point for investigating experimental signatures of high- S QSLs by adapting techniques developed for the $S = 1/2$ KHM. In particular, we want to compute the dynamical structure factor of the $S = 3/2$ KHM that can be measured in neutron scattering experiments.

Original publication: *Nat. Comm.* (2022) doi.org/10.1038/s41467-022-31503-0

Contact author: Hui-Ke Jin, Technische Universität Muenchen, Germany. huike.jin@tum.de

ILL contact: William M. H. Natori. natori@ill.fr

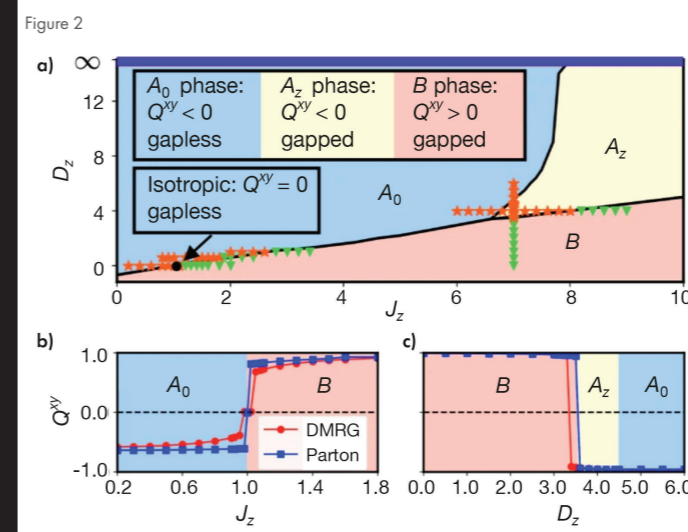
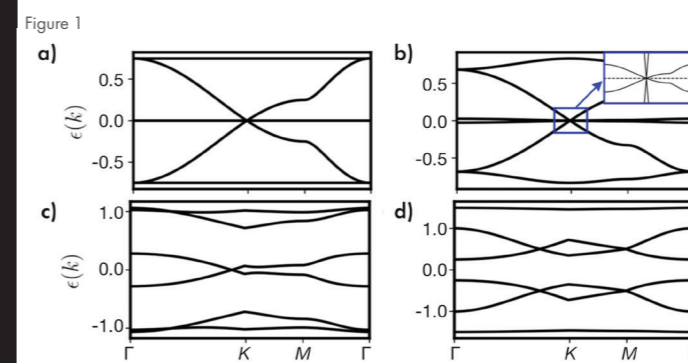


Figure 1: a) Phase diagram of the $S = 3/2$ KHM along the line $J_x = J_y = 1$ perturbed by a single-ion anisotropy D_z . b) and c) Cuts of this phase diagram showing quantitative agreement between DMRG and parton mean-field theory.

Figure 2: Band dispersion of a quantum spin–orbital liquid emerging from an exactly solvable model. Along the line $J_x = J_y = 1$, we show the dispersion of the $S = 3/2$ KHM QSLs at b) $J_z = 1$, c) $J_z < 1$ and d) $J_z > 1$.

Atomic distribution and local structure in ice VII from *in situ* neutron diffraction

Water is a fundamental substance in nature. Despite its apparent molecular simplicity, both water and its solid form, ice, show unique physico-chemical properties that are distinct from other molecular materials. One key example is a disorder of molecular orientations that accompanies spatial displacements from average positions. Ice VII, stable between 2 and 60 GPa at 300 K, is a textbook example of disordered ice and is generally represented by a simple cubic structure. In ice VII, oxygen atoms covalently bond to two hydrogen atoms distributed over four crystallographically equivalent sites with half occupancies. This structure model is called the ‘single-site model’. This model has been widely accepted to date but is also known to lead to chemically unrealistic molecular geometries. Thus, more accurate ‘multi-site’ models have been proposed to describe the real structure of ice VII. However, elucidations of the very small atomic displacements (~ 0.1 Å) are not without their ambiguities, mainly due to the technical difficulty of single-crystal neutron diffraction under pressure.

Here, we performed, for the first time, *in situ* single-crystal neutron diffraction experiments of ice VII. This work was made possible by the development of new diamond anvil cells (DACs). These enable *in situ* measurements without angular limitations, similar to samples without containers. **Figure 1** shows a DAC installed on the D9 four-circle diffractometer.

Single-crystalline specimens of deuterated ice VII were grown directly from a solution in the DAC by cyclic heating and cooling over 2 GPa. In addition to the technical improvements in measurements, we applied a maximum entropy method (MEM) analysis to reveal three-dimensional atomic distributions without the constraints of structure models like the single-site model.

Results of the MEM analysis show ring-like distributions of deuterium around the $\langle 111 \rangle$ axes, in the direction of the oxygen of hydrogen-bonded water (**figure 2**). The distance between the average oxygen site and the ring-like distribution of deuterium is shorter than a plausible covalent O–D bond length of 0.97 Å. This explains the unrealistically short O–D covalent bond derived from conventional structure analysis using the single-site model. Regarding the other atomic species, oxygens show more elongated distributions toward the O–D covalent bond (**figure 2**), which corresponds to $\langle 111 \rangle$ directions. However, the density distributions are also spread in other directions, meaning that other components are not fully excluded. The real structure of the disordered ice VII will therefore be a combination of dominant displacements toward $\langle 111 \rangle$ and some other components with variations.

Our study shows unambiguously the three-dimensional atomic distribution in ice VII, the model-free MEM approach as distinct from the single-site model highlighting its peculiar disordered structure. These displacements of oxygen and deuterium were partially proposed in previous studies, but the displacement ellipsoid conventionally

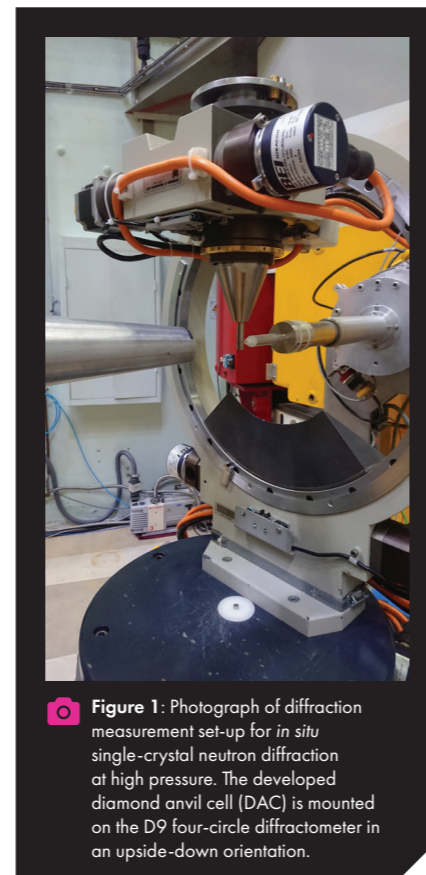


Figure 1: Photograph of diffraction measurement set-up for *in situ* single-crystal neutron diffraction at high pressure. The developed diamond anvil cell (DAC) is mounted on the D9 four-circle diffractometer in an upside-down orientation.

used in least-squares structure refinements can only approximately describe their complicated distributions.

Our findings can lead to a better understanding of the physical properties of water ice under pressure. Furthermore, the atomic distributions may also be linked to dynamic motions. The derived distributions are the time and spatial average of water molecules in different orientations. Rotation dominantly contributes to the dynamic motion in ice VII at lower pressure but is suppressed at higher pressure, followed by a crossover with translation at 11–13 GPa. The ring-like feature of deuterium is considered to be related to the molecular rotations and reflects changes in this dynamical behaviour.

Original publication: PNAS (2022)—[doi:10.1073/pnas.2208717119](https://doi.org/10.1073/pnas.2208717119)

Contact: Keishiro Yamashita, University of Innsbruck, Austria. keishiro.yamashita@uibk.ac.at

ILL contact: Oscar Fabelo. fabelo@ill.fr

Instrument: Hot neutron four-circle diffractometer D9

Wide-angle neutron spin echo provides new insight into the microscopic relaxation dynamics of glass-forming liquid

Glasses, which are macroscopically solid-like (rigid) but microscopically liquid-like (amorphous or lacking periodic arrangements), are an interesting class of materials. Despite their wide range of applications, an in-depth understanding of the physics of the glass transition is still lacking. The challenge comes mostly from the fact that upon cooling liquids towards the glass transition, the relaxation time (or viscosity) undergoes an extraordinary increase and shows increasing heterogeneity while the microscopic structure shows only minute changes. To establish a detailed atomic-level description of the complex relaxation dynamics of glass-forming liquids, direct measurement of the relaxation processes at different microscopic length scales is required—something that was impossible, or at best extremely demanding, before the recent commission of the wide-angle spin-echo (WASP) spectrometer at the ILL.

The WASP spectrometer employs anti-Helmholtz coils to allow the simultaneous measurement of the coherent intermediate scattering function (ISF)—which describes how atoms lose memory of their original arrangements—over a broad Q -range with unprecedented high data rate and accuracy.

In this work, we used WASP to investigate a prototypical ionic glass-forming liquid, $\text{Ca}_{0.4}\text{K}_{0.6}(\text{NO}_3)_{1.4}$ (CKN, glass transition temperature $T_g \approx 336$ K and liquidus temperature $T_l \approx 483$ K), over the full range of microscopic length scales. The structure

factor of CKN has a primary peak at around $Q_1 \approx 1.86 \text{ \AA}^{-1}$, originating mainly from the correlation of neighbouring nitrate ions; and presents a second broad peak at $Q_2 \approx 2.85 \text{ \AA}^{-1}$, manifesting mainly ionic oxygen–cation correlations. A pre-peak at $Q_0 = 0.8 \text{ \AA}^{-1}$ arises from the intermediate-range aggregates of nitrate ions.

Figure 1 shows representative ISFs measured on WASP fitted to a two-exponential model. A simple exponential describes the initial fast process, the atomic movements within the neighbours’ cage; while a stretched exponential function describes the slow α -process, the escape of the atoms from the cage.

Figure 2 shows the temperature dependence and Q dependence of the relaxation dynamics derived from the ISFs. The stretching exponent β is indicative of both the heterogeneity and co-operativity of the motions. For $Q \leq 2.33 \text{ \AA}^{-1}$ (left panel of **figure 2a**), the β of the low-viscosity liquid at $T > 470$ K is independent of temperature. That it decreases with decreasing temperature at $T < 470$ K is indicative of increased heterogeneity and co-operativity of the α -relaxation in the highly viscous liquid state. However, for $Q = 2.49 \text{ \AA}^{-1}$, β also decreases with decreasing temperature at $T < 470$ K, but at a much slower rate than that at lower Q s. Finally, for $Q \geq 2.60 \text{ \AA}^{-1}$ β shows no systematic change with temperature (right panel of **figure 2a**).

As characteristic of so-called fragile glass-formers, the temperature dependence of the slow α -relaxation time (τ_{slow}) cannot be described by a simple Arrhenius law with

a single activation energy. Instead, it was analysed in terms of a Vogel–Fulcher–Tammann (VFT) function, which indicates a corrugated energy landscape. **Figure 2b** shows that the parameters D and T_0 of the VFT law follow the shape of $S(Q)$ at $Q < 2.4 \text{ \AA}^{-1}$; while at $Q > 2.4 \text{ \AA}^{-1}$ D shows a rapid increase with increasing Q , and T_0 a rapid decrease, indicative of smaller deviation from Arrhenius behaviour.

Our systematic studies of highly viscous liquid states using WASP over a broad wave vector–time–temperature (Q - t - T) space revealed a crossover of the dominant relaxation mechanisms around a characteristic length of $2\pi/Q \approx 2.6 \text{ \AA}$ ($Q = 2.4 \text{ \AA}^{-1}$). Above 2.6 \AA , the relaxation dynamics show a strong temperature dependence for both the activation energy and the relaxation time distribution; in contrast, at local length scales below 2.6 \AA the dynamics are more Arrhenius-like and the relaxation time distribution is independent of temperature. These results shed new light on the evolution of the microscopic dynamics of glass-forming liquids upon cooling towards the glass transition.

Original publication: Nat. Commun. (2022)—[doi:10.1038/s41467-022-29778-4](https://doi.org/10.1038/s41467-022-29778-4)

Contact author: Y Z, Department of Nuclear Engineering and Radiological Sciences, University of Michigan, USA. yyz@umich.edu

ILL contact: Peter Falus. falus@ill.fr

Instrument: Wide-angle spin-echo spectrometer WASP

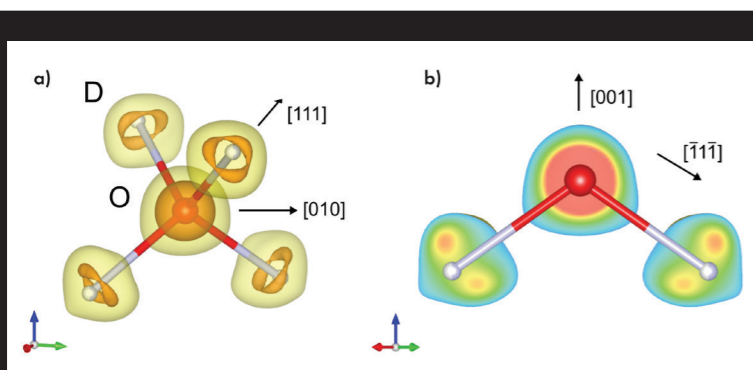


Figure 2: Distribution of scattering-length density in ice VII derived from single-crystal neutron diffraction at 298 K and 2.2 GPa, where **a**) is a cross section of **a**) on the (110) plane. The oxygens and deuteriums are illustrated as those in the single-site model where O–D = 0.97 Å, as in the water molecule, for comparison. Density decreases from red to blue.

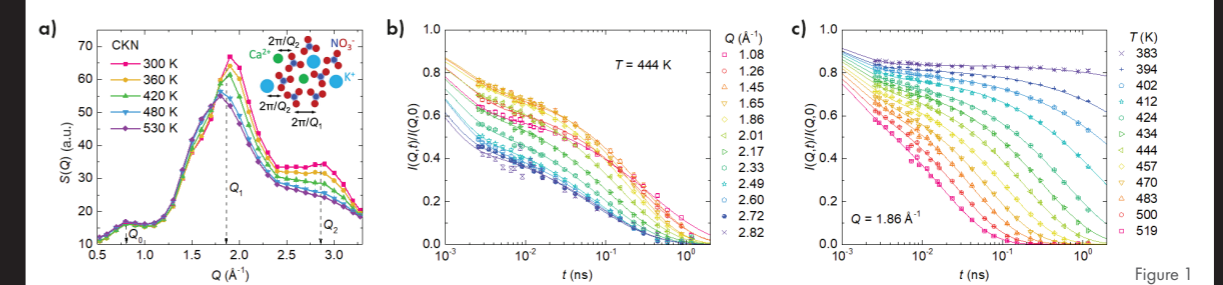


Figure 1

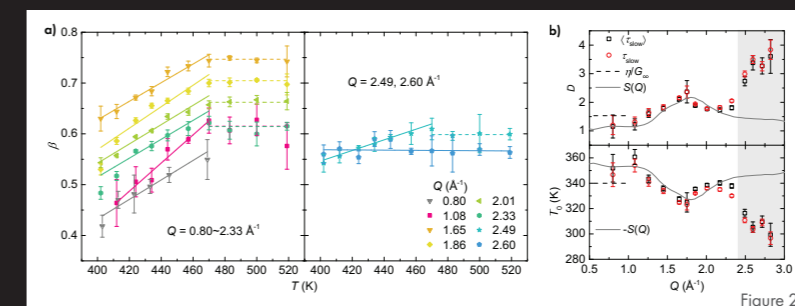


Figure 2

Figure 1: Normalised ISFs measured on WASP of liquid CKN. **a**) at $T = 444$ K for various Q s and **b**) at $Q = 1.86 \text{ \AA}^{-1}$ for different temperatures. The inset in **a**) is a schematic of the CKN structure with indicated correlation lengths.

Figure 2: **a**) Exponent β versus temperature for different Q s; **b**) Q dependence of the VFT parameters D and T_0 follow the shape of $S(Q)$ at $Q < 2.4 \text{ \AA}^{-1}$, while deviating from the prediction of $S(Q)$ at $Q > 2.4 \text{ \AA}^{-1}$ and changing towards what is indicative of smaller deviation from Arrhenius behaviour.

Which path does a particle take in a double-slit experiment?

This question is as old as quantum mechanics itself. The most well-known and probably most significant experiment in quantum physics is the double-slit experiment, in which particles are fired at a wall with two openings. Behind the slits, the intensity is recorded on a screen. While classical particles would create only two peaks, one for each slit, quantum particles create a fringe pattern which arises from the interference of both slits' contributions.

Interestingly, this pattern also builds up if the particles arrive one after the other. This is everyday business at the neutron interferometer set-up S18, which resembles the double-slit configuration. The neutron beam splits into two paths that are then superimposed and brought to interference. Given the velocity of thermal neutrons (2 km/s), the beam intensity (10^4 cps) and the size of the set-up (several tens of centimetres), it follows that there is hardly ever more than one neutron in the set-up; and still, interference is observed.

To explain this single-particle interference, one usually assumes that each particle takes both paths simultaneously. However, this interpretation can be challenged. Since a whole ensemble of particles is required to observe the interference pattern, and since particles can be detected only as a whole, there are interpretations of quantum mechanics that stick to well-determined trajectories for individual particles. The de Broglie-Bohm theory, for example, interprets the wave function as a pilot wave that explores the possibilities along both paths while the particle itself is assumed to travel only one or other path. The particles would be statistically distributed over both paths. With an experiment performed last year on S18 we were able to distinguish between these interpretations.

Direct observation of the particles in the paths is impossible, as it would destroy the interference due to complementarity of which-way information and the visibility of interference. Instead, one takes a 'weak measurement'. The neutrons are marked in one path by a small spin rotation, and by analysing the spin in the exit beams one extracts the 'weak value' of the neutron presence in the paths. To maintain (nearly) full interference the spin rotation angle α must be small, which in turn requires the which-way information to be collected over many measurements. Consequently, the path presence obtained is again

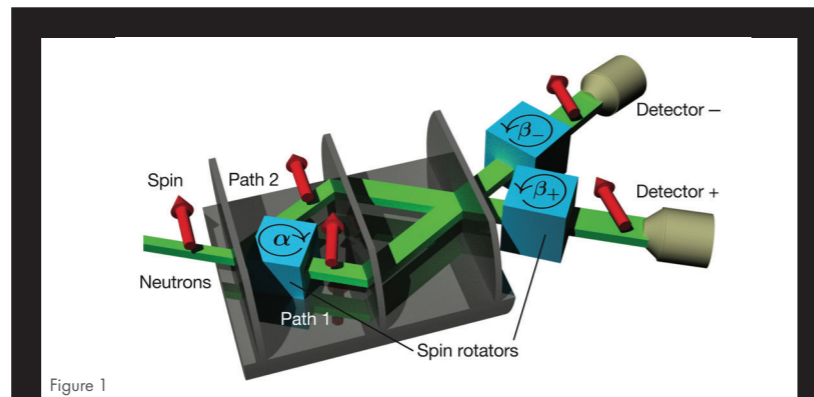


Figure 1

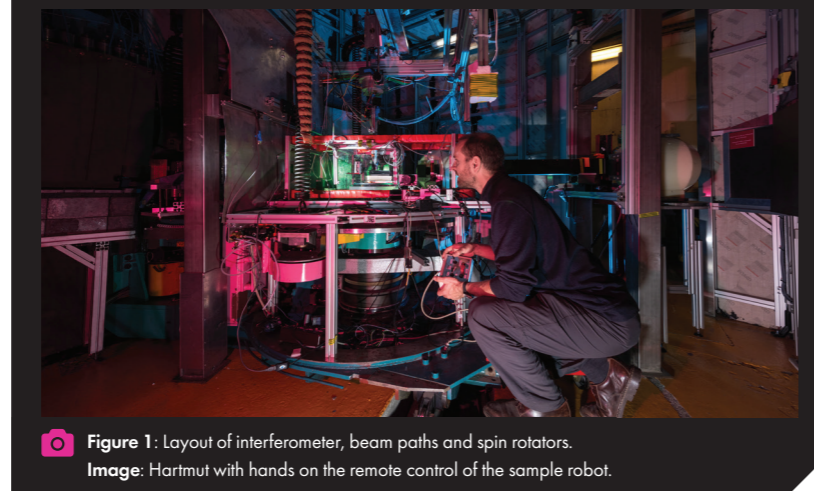


Figure 1: Layout of interferometer, beam paths and spin rotators. Image: Hartmut with hands on the remote control of the sample robot.

a collective entity and does not say where an individual neutron has been.

In our experiment we go a step further and compensate for the α rotation with a counter-rotation β in the exit beams (cf. figure 1). The angle ratio directly yields the path presence. If a back rotation by $\beta = 2/3 \alpha$ is necessary to obtain the initial state, then only 2/3 of the neutron has experienced the α rotation in path 1 and we conclude that the neutron was to 2/3 in path 1 and to 1/3 in path 2. Importantly, under certain conditions the compensation becomes ideal, meaning that really all neutrons return to the initial spin state. Then the variance vanishes, and the ensemble average of the path presence is valid for each individual particle.

To summarise, we prove that (and quantify how) individual neutrons are distributed over two paths while full visibility of interference is maintained. Does this contradict complementarity? No, because we perform a conventional weak measurement for determining the path presence. Once we have this information we can verify it on subsequent neutrons, and verification of an estimate can be error-free and non-disturbing.

	Path 1	Path 2	
Initial probabilities	$p_1 = 4/5$	$p_2 = 1/5$	
Initial amplitudes	$\alpha_1 = 2/\sqrt{5}$	$\alpha_2 = 1/\sqrt{5}$	
	Probability	Presence in path 1	Presence in path 2
Exit +	$p_+ = 9/10$	$\omega_{1+} = 2/3$	$\omega_{2+} = 1/3$
Exit -	$p_- = 1/10$	$\omega_{1-} = 2$	$\omega_{2-} = -1$

Table: Path presence ω measured in the experiment using an asymmetric 4:1 beam splitter. The two interferometer exits '+' and '-' represent constructive and destructive interference, respectively. Being a weak value, ω depends on the exit. The 'anomalous' weak values ω_{1-} and ω_{2-} might surprise our common sense. Nevertheless, they are required to reproduce the original path probabilities by averaging over the '+' and '-' sub-ensembles: $p_1 = p_+ \omega_{1+} + p_- \omega_{1-}$ and $p_2 = p_+ \omega_{2+} + p_- \omega_{2-}$.

Original publication: Phys. Rev. Lett. (2022)–doi:10.1103/PhysRevResearch.4.023075

Contact author/ILL contact: Hartmut Lemmel, TU Wien. hartmut.lemmel@tuwien.ac.at

Instrument: Neutron interferometer S18

Constraining axion-like dark matter using cold neutrons

Dark matter is a postulated form of matter that is not directly visible but instead interacts via gravity. It makes up roughly 84 % of the matter content in our universe. So far, no dark matter model has been experimentally verified. Nevertheless, the axion and a more general class of axion-like particles (ALPs) remain promising candidates. We constrained the possible existence of axion-like dark matter with a measurement performed at the cold neutron beam facility PF1B, using the Beam EDM apparatus developed at the University of Bern (Switzerland).

The coupling of axions and ALPs to gluons is a common feature in many theories that go beyond the standard model of particle physics. One consequence of this coupling is that an oscillating ALP field induces a proportionally oscillating electric dipole moment (EDM) of the neutron. The parameter space of ALPs is defined by their mass and coupling constant. It is restricted by various astrophysical and cosmological constraints and has been scrutinised in three recent laboratory experiments.

In our new experiment, we applied Ramsey's method of separated oscillatory fields to cold neutrons. With this technique, neutrons act as a spin clock at their Larmor precession frequency in superimposed magnetic and electric fields. We measured this frequency precisely and examined it for the slightest periodic fluctuations that the interaction with the ALPs could cause.

The experimental apparatus employs two parallel beams of polarised cold neutrons, which enter a homogeneous and stabilised vertical 220 μ T magnetic field. Passive magnetic shielding surrounds the entire set-up. Two radio frequency spin-flip coils, one before and one after the three-metre long electric field region, induce resonant 90° flips of the neutron spin. In the electric field region (35 kV/cm), the interaction of the neutrons with the ALP field induces an oscillating EDM signal. Downstream of the set-up, a neutron spin analyser spatially separates the two spin states of each beam before they are counted in a 2D pixel detector. Photos of the apparatus producing the electric field, including the interior of the vacuum beam pipes with the electrodes, are shown in figure 1.

We performed a fast and continuous measurement of the neutron EDM. The analysis presented used 24 hours of data with a sampling rate of 4 kHz, i.e. one EDM value every 0.25 ms. The data were recorded in September 2020 and are publicly available. Besides having a significant amplitude over the background noise level, an oscillating EDM signal induced by ALPs must disappear if no electric field is present. This way, noise or spurious signals from external sources can be excluded.

Overall, no significant oscillating signal was found. Thus, an upper limit on the

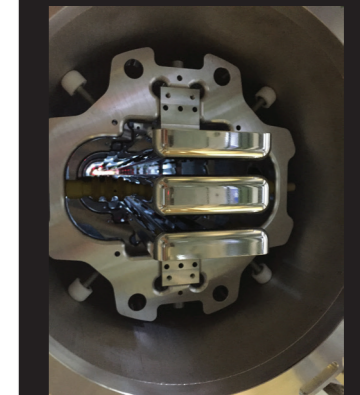
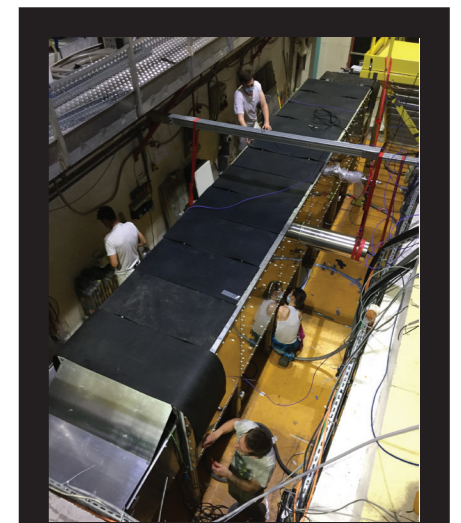


Figure 1: Top: Installation of the Beam EDM apparatus at the cold neutron beam facility PF1B. Bottom: Electrodes inside the vacuum beam pipe

ALP-gluon coupling could be derived, constraining a mass region covering almost eight orders of magnitude. Figure 2 shows the exclusion graph we obtained of the coupling as a function of ALP mass and frequency, respectively. Our experiment substantially extends the exclusion region accessible through laboratory experiments to higher frequencies. Indeed, a large part of the ALP-dark matter parameter space could be excluded, and future EDM searches may extend this even further.

Original Paper: Phys. Rev. Lett. (2022)–doi:10.1103/PhysRevLett.129.191801

Contact author: Ivo Schulthess, University of Bern (Switzerland). ivo.schulthess@lhep.unibe.ch

ILL author: Torsten Soldner. soldner@ill.fr

Instrument: Cold neutron facility PF1B

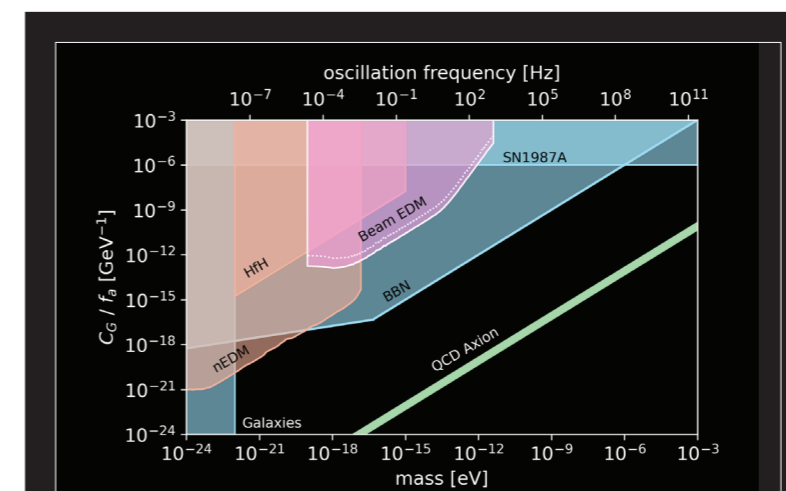


Figure 2: Limits on the ALP-gluon coupling are shown as a function of the former's mass or frequency. The shaded areas are exclusion regions from cosmological and astrophysical observations (blue) and laboratory experiments (orange). The black outlines with the pink area mark the exclusion region found in this work (labelled Beam EDM). The green line indicates where the axion would solve the Strong CP problem of quantum chromodynamics (QCD).



Facility update

© L. Thion

The ILL20–23 programme and its long shutdown activities

In 2020 the ILL launched its multi-annual ILL20–23 programme, which combines a major upgrade of the instrument suite (*Endurance*) with security and safety work on the reactor. ILL20–23 is being conducted on a master resource-loaded programme schedule, the aim being to co-ordinate instrumentation work and reactor activities during long shutdowns whilst securing the maximum number of reactor cycles for our users. Once successfully completed, the programme will provide the scientific community with a fully modernised suite of world-class instruments together with a reliable supply of neutrons. The ILL will effectively be a brand new installation, ready to operate for the decade to come.

As part of the ILL20–23 programme, the most recent 2021–2022 long reactor shutdown period has been crucial. Dozens of ILL employees have been involved in what has been a particularly intense period. The work has called for concerted effort and goodwill on the part of our staff within the Projects and Techniques (DPT) and Reactor (DRe) divisions, together with enormous technical and manpower support from the Science Division (DS). We should not forget that this shutdown work began while the ILL was still under COVID restrictions, making working conditions and close teamwork more challenging than it might otherwise have been.

At the time of writing, the reactor has just restarted and we have resumed our scientific user programme with our fully modernised H24 guide and instrument suite as well as a number of completed independent instrument projects. Broadly speaking the ILL20–23 programme is on time and on budget, with all our technical objectives successfully completed.

Beam tubes, guides renewal and construction works

The most critical project during the past 16 months has been the replacement of the H1–H2 beam tube and in-pile neutron guides that allow thermal and cold neutrons to be extracted and transported to the instruments in the ILL7 guide hall.

To replace the H1–H2 beam tube, a huge amount of work had to be done in the reactor building. This included dismantling

330 metres of guides in pile and in the level C casemate up to the reactor containment double wall, to make way for the replacement. This also gave us the opportunity to replace all the other pool guides. These must be changed every 10 years because the glass they are made of deteriorates over time, due to their exposure to radiation from the reactor core. Although a huge operation in itself, doing this gave us the opportunity to modernise and renew infrastructure such as the H1–H2 pool at level C, which provides biological shielding for beam extraction, as well as the guide system for crossing the containment double wall (**C5 guide system**) which feeds through the outer reactor wall.

The latter new design has improved reactor safety in the case of an exceptional seismic event and associated possible major flooding, ensuring our compliance with the highest safety standards and guaranteeing the longevity of our key neutron delivery infrastructure. This part of the work required the complete replacement of an additional 50 metres of neutron guides. The project as a whole was completed successfully and on time, in accordance with quality procedures agreed with the ASN.

In early 2022, much of the ILL7 guide hall was excavated down to the river bed of the Grenoble valley, in preparation for the new double guide H24 and triple guide H15 and their associated nine new or refurbished instruments. Reconstruction began promptly, with extensive concrete landscaping carried out to house the new guide and instrument suites for both the H24 and H15 projects. The civil engineering work has been carried out in phases, beginning with the new D10+ zone and the H24 dual guide. Subsequent phases have followed roughly in instrument order along the Chartreuse side of the guide hall towards XtremeD, IN13+ and the future area for FIPPS. A similar situation can be seen on the Vercors side of the guide hall, with the dismantling of the old H1 casemate to pave the way for civil engineering work for the H15 triple guide and its instruments suite: D007, D11+, SHARP+ and SAM.

The construction of the new cold guide casemate (**H1 casemate**), a critical prerequisite for restarting the user programme in ILL7, presented a major challenge. Nevertheless, this project too was successfully completed, on time, by the end of 2022. This 300 m² structure, made of concrete, lead and steel, is

vital for ensuring the safe distribution of neutrons to users of the existing cold guides. Furthermore, it has been specially designed to accommodate three additional future branches of the guide H15, which will supply neutrons to the new H15 instruments.

During the spring and into the summer of 2022, installation of the first instrument components, such as the primary spectrometer shielding for D10+ and XtremeD and the instrument zone separation walls, began. By the beginning of the summer, work on the new H1 steel casemate roof could begin and the new foundation pillars for the D11 detector tank could be poured. By the end of the summer, work then began on reinstalling the IN13 and CT2 instruments, while the new floors for FIPPS and SHARP+—at the ends of the H24 and H15 beamlines, respectively—were prepared.

Through the autumn and into winter 2022–23, instrument mounting proceeded quickly, with D10+, IN13, XtremeD and CT2 all beginning to look like completed neutron instruments ready to start their cold commissioning. At the same time, the D11 detector tube was moved into its new position and the SHARP+ flight chamber was delicately ‘air-lifted’ though the roof of ILL7 into its new position at the end of the guide hall on its Vercors side.

Meanwhile, following the successful replacement of the H1–H2 beam tube in the reactor building, reassembling the great puzzle of the 330-metre long guides got underway at the end of autumn 2022. Realigning the whole neutron distribution feeding the ILL7 guide hall with a positioning accuracy of the order of a few hundredths of a mm in just two months was a challenge: one that we had to rise to if we were to be able to reinstall the eleven H1–H2 safety valves, the prerequisite authorising fuel element loading, perform the final tests and restart the reactor.

The process began with the flight of the so-called ‘Pink Housing’ across level C to the reactor core: the very delicate handling of this 700 kg piece of machinery loaded with 35 metres of fragile glass guides that will give birth to the ILL7’s neutron delivery system. In early December we were able to reinstall the subsequent guide units within the narrow space of the level C pool (about 15 m² for 60 m of guides), and in the following weeks to connect them to the last sections already installed across the reactor containment double wall.

New instruments ready for operation

On the Chartreuse side of ILL7, the new suite of H24 instruments will begin commissioning with the restart of the reactor in March 2023. In comparison with the old D10 instrument we are expecting gains of an order of magnitude on the new D10+ single-crystal diffractometer, thanks to the new detector and increased divergence, guide and monochromator size. Gains in intensity are expected on IN13+ too, primarily due to the performance of the new H24 guide, coupled with a new temperature-gradient monochromator. New capabilities and capacity will also be available with the new CRG powder and single-crystal diffractometer XtremeD, while the end of the new H24 guide will make way for the future relocation of the fission fragment spectrometer FIPPS. This will give the instrument more space, reduced background and, most importantly, a stable and intense neutron beam.

The cold neutron instruments on the Vercors side of ILL7, with the exception of the H15 instruments, are also now ready to restart. The work on H15 has been planned in such a way as to allow construction of the out-of-casemate H15 guide and instruments to continue during reactor operation in 2023. The next long shutdown, scheduled for the beginning of 2024, will allow the final in-casemate installation of the new H15 guides. This will at last connect the new guide to its new instrument suite, ready for commissioning and user operation during the second half of 2024. We expect huge gains in performance from instruments such as D007 and SHARP+ (CRG) due to the new high-performance H15 guide, dedicated focusing guide and beam optics, and improved or larger detectors. Additionally, D11 should regain its theoretical brilliance, to match that of D22 and D33, as should the new CRG SANS instrument SAM.

Several other instrument projects will also begin commissioning and enter the user programme in 2023. The neutron imaging instrument NeXT is a fully rebuilt instrument with two measurement stations allowing state-of-the-art N-imaging with advanced contrast techniques, high spatial resolution, intense neutron flux and combined X-ray imaging. The cold neutron diffractometer and wide-angle scattering instrument D16 now has a fully renewed secondary spectrometer; this contains a new position-sensitive detector that covers four times the solid angle of the previous detector, allowing for more rapid measurements over an extended q-range.

Although already commissioned in 2020, the thermal time-of-flight spectrometer PANTHER’s performance will increase yet further thanks to its new cascade of five background choppers. And SuperSUN will finally produce its first ultra-cold neutrons after an extended and complex instrument project and commissioning.

We have also been able to launch several new instrument upgrade projects, including a new banana detector for the D20 powder diffractometer due to be installed in 2024. And finally, the MARMOT project will provide multiplexed energy and angle analysis on the cold neutron TAS instrument Thales, while the wide-angle spin-echo instrument WASP will receive its full complement of detectors.

An ever safer reactor: an overview

Over the last few months the ILL has had to satisfy many commitments vis-à-vis the French nuclear safety authority, the ASN, in addition to carrying out mandatory maintenance work.

The long reactor shutdown was due to last 16 months: 14 months of designated work and two months to cover risks. Most major milestones were completed on time, thanks to the high motivation of ILL staff. While some activities proceeded smoothly, we faced some unexpected technical difficulties and some delays in procuring raw materials. Nevertheless, we were able to contain these unanticipated setbacks within our two-month margin and stick to our overall 16-month deadline.

The many activities carried out within the Reactor Division include the following major operations:

- replacement of the H1–H2 beam tube—the most complex beam tube ever made, it extracts the cold and thermal neutrons feeding all instruments in the main ILL experimental hall. One of the most difficult and critical operations during the long shutdown, it was carried out faultlessly and without delay.
- replacement of the reactor core chimney—a highly critical part that not only houses the fuel element in the core but also channels its cooling. One of the most important milestones in the schedule, this activity was completed successfully and earlier than planned.
- reinforcement of the Fresh Air Intake—to avoid the risk of damaging the reactor containment in the event of an earthquake, the old concrete

building has been demolished and replaced with a lighter structure.

- testing of the CRU (emergency core reflood system) safeguard system—for even safer installation, this system will ensure that the fuel element remains under water even in a worst-case scenario.
- testing of the leak tightness of the reactor building containment—an activity that must be carried out every five years, in accordance with the regulations. The containment comprises an outer metal dome and an inner concrete wall separated by an air space known as the annular space and maintained at overpressure. No leak was detected, indicating the success of our containment capability and giving us a green light for the years ahead.
- cleaning of the ILL’s old detritiation facility—involving most of the services in the Reactor Division, the aim of this operation is to remove the tritiated gas still present in the detritiation building, by 2025. The idea is to design a new process for the catalytic recombination of tritiated deuterium gas with oxygen in order to produce heavy water for the primary circuit.

As well as the intensive work carried out during the shutdown, the ILL’s progress on the fuel cycle continues with its participation in the HERACLES programme. The aim is to move to using low-enriched uranium (LEU) within the next ten years. Work on a feasibility study review at the end of 2023 is ongoing.

Finally, as has been the case for the last two years the ILL’s relations with the ASN continue to be good. This is evident from the confidence expressed by the regulator at our annual review in March 2022. Feedback received from the 2022 inspections has been positive overall.

The ASN has issued its final decision on the ten-year safety review, validating the list of safety modifications to be carried out and authorising the ILL to continue to operate for the next 10 years.

Contributors: Jérôme Beaucour, Charles Dewhurst, Jérôme Estrade, Benjamin Giroud and Catherine Menthonnex.

Endurance gain matrix

Table 1: Matrix of performance and capability gains as a result of the Endurance project.

Instrument/project	Flux	Background reduction	Detector, $\Delta\Omega$	Measurement range (q, E)	Capabilities, features, options	Science	Status
H24 projects							
D10+	x5	–	x2	–	<ul style="list-style-type: none"> Flux x5 on the sample due to the new H24 guide and larger, modernised monochromators Gain x2 in detector efficiency with the new detector 	<ul style="list-style-type: none"> Shape-memory alloys High-Tc Superconductors Molecular magnets Magnetocaloric materials Functional materials 	Commissioning
IN13+	x4	–	–	–	<ul style="list-style-type: none"> Modernisation and re-siting onto the new H24 guide A new thermal gradient monochromator and deflector to capitalise on the increased flux of the new H24 guide 	<ul style="list-style-type: none"> Internal dynamics of biological macromolecules Applications in biology, medical science, chemistry, physics 	Commissioning
XtremeD (CRG)	–	–	–	–	<ul style="list-style-type: none"> Powder and single-crystal diffractometer Expected performance comparable with that of D20 	<ul style="list-style-type: none"> Diffraction measurements under extreme conditions Applications in crystallography, geosciences, magnetism 	Commissioning
H15 projects							
D007	x20	✓	–	–	<ul style="list-style-type: none"> Large, dedicated end-of-guide on renewed H15 guide Full renewal of primary spectrometer Unique instrument with as-yet-to-be-unleashed capabilities 	<ul style="list-style-type: none"> TOF spectroscopic studies Magnetic short-ranged order Separation of magnetic/nuclear scattering Separation of coherent incoherent scattering Spectrometry 	Installation
Sharp+ (CRG)	x5	✓	x2	✓ (q,E)	<ul style="list-style-type: none"> High performance cold-neutron TOF spectrometer comparable with IN5 Massive gains over existing IN6 with increased detector area, dedicated H15 end-of-guide position 	<ul style="list-style-type: none"> Magnetic excitations Structure/dynamics of liquids and glasses Spectroscopy in solid-state physics and chemistry Structure/dynamics of biological systems Structure/dynamics of soft-condensed matter 	Installation
SAM (CRG)	x5	–	–	–	<ul style="list-style-type: none"> Additional SANS capacity and capability (4th SANS at ILL) MEIZE capability option 	<ul style="list-style-type: none"> Broad applicability in diverse science domains (soft matter, biology, physics, materials and magnetism) 	Installation
Independent projects							
Panther	x2	x10	x3	✓ (q,E)	<ul style="list-style-type: none"> Double-focus mono, 2D PSD Enhanced background suppression Unique high-energy TOF spectroscopy 	<ul style="list-style-type: none"> Magnetic excitations in quantum and/or frustrated magnets, spin, crystal-field excitations Lattice dynamics Materials for energy Complex molecular systems 	Complete
FIPPS	–	x1.5 (anti-Compton shields)	–	✓ (γ)	<ul style="list-style-type: none"> New instrument, new capability Prompt γ fission 	<ul style="list-style-type: none"> Structure of neutron-rich nuclei (n, γ) reaction on stable or radioactive targets 	Complete
Rainbows	x10	–	–	–	<ul style="list-style-type: none"> Renewed focusing guide to maximise 'coherent summing' method for specular reflectivity measurements 	<ul style="list-style-type: none"> Fast kinetics Smaller samples Electro- and photo-chemistry Oxidations and other reactions 	Complete
IN5+/H16 (CPER)	> x3	✓	–	✓ (q,E)	<ul style="list-style-type: none"> H16 guide and instrument focusing guide renewal Access to shorter λ, higher E Flagship instrument pushing the boundaries further 	<ul style="list-style-type: none"> Quasi-elastic studies in amorphous, biological and liquids systems Phonons in classical and quantum crystals Excitations in molecular nanomagnets Excitations in quantum liquids Classical and quantum magnetisms 	Complete

Instrument/project	Flux	Background reduction	Detector, $\Delta\Omega$	Measurement range (q, E)	Capabilities, features, options	Science	Status
D3-Liquids (CPER)	–	–	x10	✓	<ul style="list-style-type: none"> Higher order and background suppression Improved flux and polarisation Multiplexed analysis Unrivalled thermal TAS spectroscopy 	<ul style="list-style-type: none"> Study of disordered materials including liquids, glasses, quasi-crystals and nano-sized systems, from fundamental research to health and environmental sciences, or applied research 	Complete
IN20-Upgrade	x2	✓	x10 (multiplex analyser)	✓ (q,E)	<ul style="list-style-type: none"> Higher order and background suppression Improved flux and polarisation Multiplexed analysis Unrivalled thermal TAS spectroscopy 	<ul style="list-style-type: none"> Superconductivity, high-Tc pnictides Orbital/charge transfer phenomena Exotic excitations/quantum magnets Strong spin-orbit coupling phenomena 	NVS: Complete Mono/Analyser: In progress Multiplex: Not started
SuperSUN	UCN density x7	–	–	–	<ul style="list-style-type: none"> A source of ultracold neutrons with UCN density x7 the previous record 	<ul style="list-style-type: none"> PANEDM collaborative experiment to install on SuperSUN source for world record measurements of the neutron electric dipole moment 	Commissioning
DALI	x3 LADI	–	–	–	<ul style="list-style-type: none"> Higher protein crystallography capacity Higher resolution mode Best-in-world instrument High-impact science 	<ul style="list-style-type: none"> Determination of enzyme mechanisms Drug design studies 	Complete
Marmot (Thales)	–	–	x25 (multiplex analyser)	✓ (q,E)	<ul style="list-style-type: none"> An optimised multiplexed analyser detector for ThALES Simultaneous multi-channel energy analysis over a wide angular range 	<ul style="list-style-type: none"> Correlated electronic systems and exotic quantum spin systems such as non-conventional superconductors, strongly frustrated, low dimensional or disordered systems 	Prototype OK: In progress
NeXT	✓	✓	✓	✓	<ul style="list-style-type: none"> New capability and public neutron imaging instrument White-Monochromatic beam and various contrast options Improved spatial resolution 	<ul style="list-style-type: none"> Geometrical measurements with complex sample environments Quantitative measurements of sample evolutions Combination of multiple techniques: neutron and X-ray, grating interferometry, polarised neutrons, etc. 	Commissioning

Detectors and collimations							
D16 Detector	–	–	x4.5	✓ ($\Delta q \times 4.5$)	<ul style="list-style-type: none"> Modern, larger, high count-rate detector Larger solid angle and dynamic q-range Unique cold neutron diffractometer 		Commissioning
D20 Detector	–	–	–	–	<ul style="list-style-type: none"> Critical replacement of ageing detector Workhorse, high-demand, impact instrument 		In progress
D11 Detector	–	–	x2	✓ ($\Delta q \times 1.5$)	<ul style="list-style-type: none"> Large, modern, high count-rate detector Workhorse instrument, necessary upgrade 		Complete
D22++ Detector	–	–	x10	✓ ($\Delta q \times 10$)	<ul style="list-style-type: none"> Large, modern, high count-rate detector for extended q-range Flagship instrument with cutting-edge science pushing the limits of SANS 		Complete
D11 Collimation	x1.4	✓	–	–	<ul style="list-style-type: none"> Flux gain due to new H15 guide Replaces unreliable, difficult maintenance, optically poor collimation Removes parasitic scattering and reflections 		Installation

Other projects							
Instrument/project	Capabilities, features, options				Science		Status
NESE	Continued stimulus and new capabilities in sample environment for neutron scattering measurements across all instruments and scientific domains				<ul style="list-style-type: none"> Sample environment is essential in ensuring innovative and successful use of beamtime 		In progress
BASTILLE	Continued stimulus, new capabilities and maintenance of scientific software for data treatment and analysis				<ul style="list-style-type: none"> Automatic and live data reduction Data analysis and computer modelling 		In progress

INSTRUMENT LIST – FEBRUARY 2023

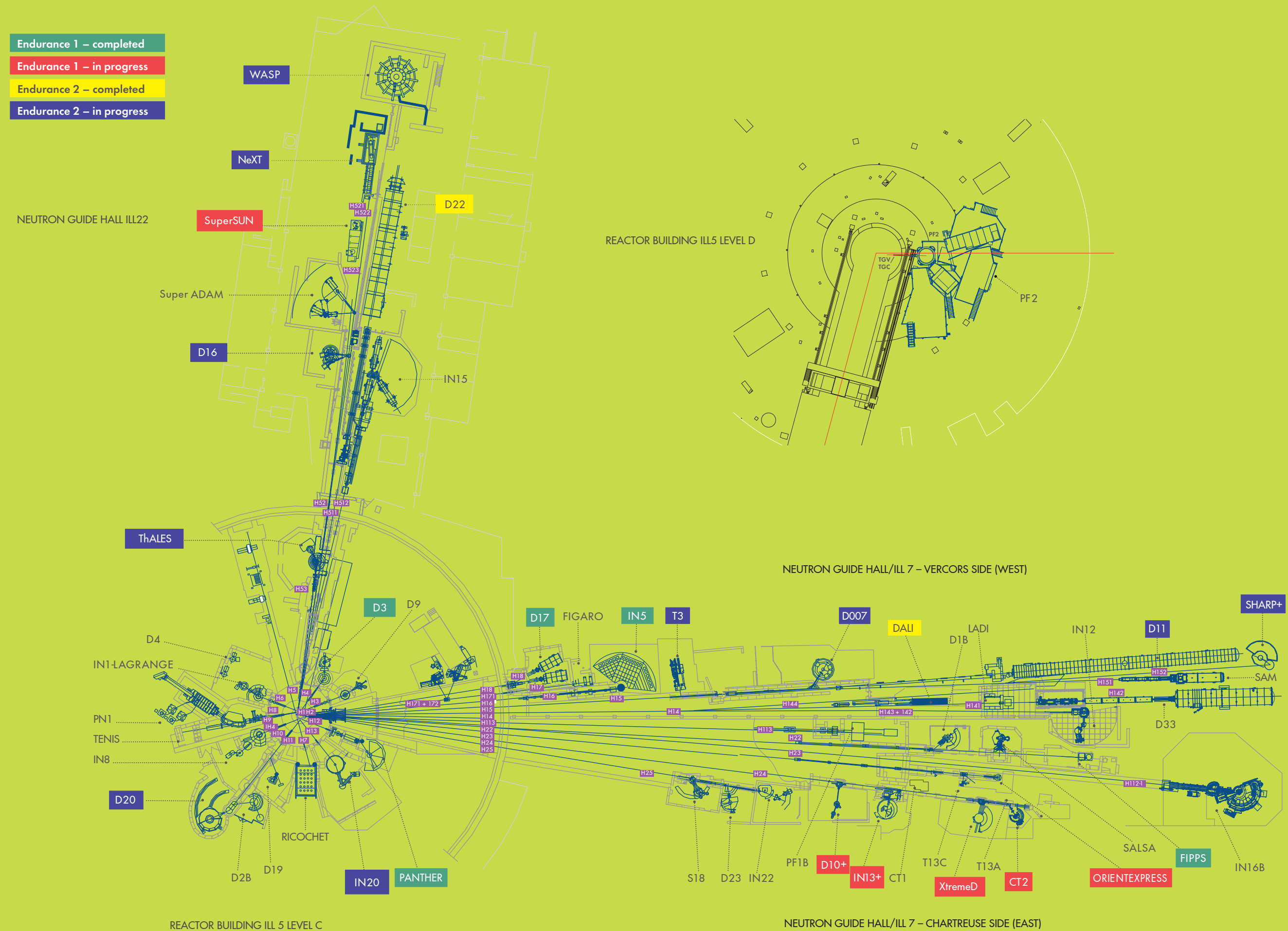
ILL INSTRUMENTS		
D2B	powder diffractometer	operational
D3	single crystal diffractometer	operational
D4 (50 % with IN1-LAGRANGE)	liquids diffractometer	operational
D7	diffuse-scattering spectrometer	will be replaced by D007
D9	single crystal diffractometer	operational
D10	single crystal diffractometer	operational
D11	small-angle scattering diffractometer	not operational
D16	small momentum-transfer diffractometer	operational
D17	vertical reflectometer	operational
D19	single crystal diffractometer	operational
D20	powder diffractometer	operational
D22	small-angle scattering diffractometer	operational
D33	small-angle scattering diffractometer	operational
DALI	quasi-laué diffractometer for biological macromolecules	operational
FIGARO	horizontal reflectometer	operational
FIPPS	fission product prompt gamma-ray spectrometer	operational
IN5	time-of-flight spectrometer	operational
IN8	three-axis spectrometer	operational
IN15	spin-echo spectrometer	operational
IN16B	backscattering spectrometer	operational
IN20	three-axis spectrometer	operational
LADI	Laue diffractometer	operational
LAGRANGE (50 % with D4)	neutron vibrational spectrometer	operational
PANTHER	time-of-flight spectrometer	operational
PF1B	neutron beam for fundamental physics	operational
PF2	ultracold neutron source for fundamental physics	operational
PN1	fission product mass-spectrometer	operational
SALSA	strain analyser for engineering application	operational
SuperSUN	ultracold neutron source for fundamental physics	commissioning
ThALES	three-axis spectrometer	operational
WASP	wide-angle spin-echo spectrometer	operational

CRG INSTRUMENTS		
D1B	powder diffractometer	CRG-A operational
D23	single crystal diffractometer	CRG-B operational
IN12	three-axis spectrometer	CRG-B operational
IN13+	backscattering spectrometer	CRG-A commissioning
IN22	three-axis spectrometer	CRG-B operational
SHARP+	time-of-flight spectrometer	in construction
SuperADAM	reflectometer	CRG-B operational
S18	interferometer	CRG-B operational

JOINTLY FUNDED INSTRUMENTS		
NeXT (75 %)	imaging instrument	operated with Ni-Matters composed of HZB, UGA and ILL

TEST AND CHARACTERISATION BEAMS	
CT1, CT2	detector test facilities
CYCLOPS	Laue diffractometer
OrientExpress	Laue diffractometer
TENIS	neutron irradiation position
T3	neutron optics test facility
T13A, C	monochromator test facility

Details of the instruments can be found at <https://www.ill.eu/users/instruments/instruments-list>



The instrument facilities at the ILL are listed in the table on the left and shown in the plan on p37. In addition to the ILL instruments, there are 8 Collaborative Research Group (CRG) instruments.

CRGs can build and manage instruments at the ILL to carry out their own research programmes.

There are currently two different categories of CRG instrument:







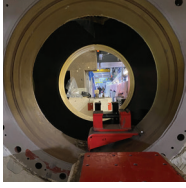






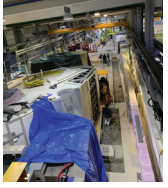

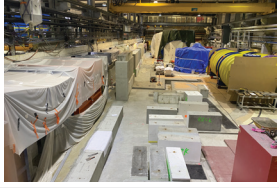

CRG-A category: the external group leases an instrument owned by ILL. They have access to 50 % of the beamtime; for the remaining 50 % the instrument is made available for the ILL's scientific user programme.

CRG-B category: the external group owns its instrument and retains 70 % of the available beamtime, supporting the ILL programme for the other 30 %.

Details about the framework of operation of CRGs can be found at <https://www.ill.eu/users/instruments/crgs>

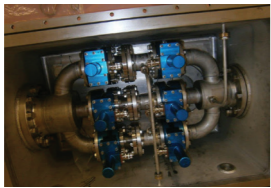








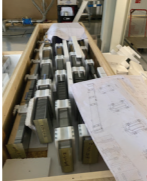






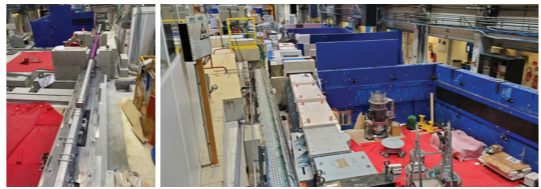







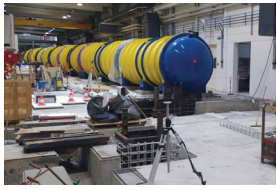
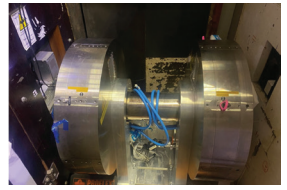
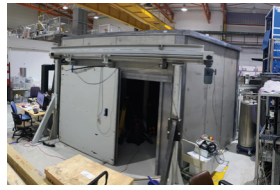


The ILL makes available to scientists a suite of state-of-the-art instruments, which are constantly upgraded.

LONG SHUTDOWN WORK TIMELINE

	Oct 21	Nov 21	Dec 21	Jan 22	Feb 22	Mar 22	Apr 22	May 22	Jun 22
REACTOR SAFETY AND MAINTENANCE	The work on the replacement and seismic reinforcement of the fresh air intake lasted more than a year and was completed in December 2022								
	Reactor shutdown 			Removal of H1-H2 beam tube. Maintenance of safety valves 	Cutting of H1-H2 beam tube 		Installation of new H1-H2 beam tube. Reinforcement of protective housing of reactor circuits 	Replacement of reactor core chimney 	
ENDURANCE									
H1-H2 works		Dismantling of H1-H2 guides in pile and in casemate Dismantling of Pink Housing		Dismantling of H1-H2 guides reactor wall pass-through	Installation of new seismically resistant containment wall penetrations for H1-H2 guides				
H24 works									
	Civil engineering work: removal of old instruments and structures and preparation of new foundations and future flooring			Installation of 35 metres in parallel to civil	of dual guide H241/242 in casemate H2 in guide hall ILL7, engineering work for various instruments in guide hall		Assembly of H241/242 guide support structures, installation and alignment of guides (upstream outside casemate H2)		
H15 works									
	Dismantling of casemates H14, H15 and H16 and associated instruments		Laying of foundations for future guide H15	Laying of flooring for instruments D11+, SAM and SHARP+	Installation of central wall of cold guide casemate				
									
Other projects								Civil engineering work and start of installation of tomography stations NeXT/MOTO 	

>> continued

LONG SHUTDOWN WORK TIMELINE continued

>> continued	Jun 22	Jul 22	Aug 22	Sep 22	Oct 22	Nov 22	Dec 22	Jan 23	Feb 23	
REACTOR SAFETY AND MAINTENANCE	The work on the replacement and seismic reinforcement of the fresh air intake lasted more than a year and was completed in December 2022									
	CRU: Qualification of emergency core reflood system 	Reinforcement of gaseous effluent outlet pipe 	Fire protection – many improvements throughout the year 	Complete renewal of H1–H2 pool lining 	Completion of H1–H2 beam tube sealing 	Installation of “Carter Pink” housing 	Preliminary clean-up of ILL’s old detritiation facility. Preparation of anchor points for replacement of trolley on polar crane on Level D 	Modifications to instrumentation and control throughout the shutdown 	Installation of H1–H2 safety valve 	
ENDURANCE										
H1–H2 works		Preparation of new H1–H2 guides 		Preparation of in-pile guides 		Transfer of “Carter Pink” housing 	Installation of guides in reactor pool 		Installation of guides in casemate on Level C 	
H24 works	Installation of XtremeD monochromator shielding 	Alignment of world’s first borated aluminium guide enabling significant space savings (no need for housing around it) 	Construction of biological shielding of experimental areas and installation of H24 instruments 						Completion of installation of D10+ 	View of new instruments of double guide H24 
H15 works		Creation of concrete blocks to support future guide H15 in cold guide casemate 		Installation of walls of new cold guide casemate 	Installation of roof of new cold guide casemate 		Installation of HDPE shielding in cold guide casemate (reduction of instrument background) New cold guide casemate and preparation of future secondary H15 guide sections (Jan 23) 		Transporting of main beam shutter of primary H15 guide to cold guide casemate 	
Other projects										
		Transfer of D11 detector tube to its new site 	Installation of PANTHER background choppers 	Installation of instrument casemate for NeXT 	Moving of SHARP+ time of flight chamber 					
										



Industry highlights

© L. Thion

Neutron applications for the microelectronics industry

Cutting-edge research techniques are key to maintaining industrial competitiveness in a knowledge-based society. For a facility like the ILL, working with industry demonstrates its relevance to society in addition to generating publishable results and income streams from the development of business-critical proprietary measurements. The Industry Liaison Unit (ILU) at the ILL captures pre-competitive research of industry relevance, develops long-term collaborations with industry and research technology organisations (RTOs), and promotes proprietary use of beam time by industrial clients. The specific challenge with neutrons is that while they offer unique insights into materials, devices and processes they are not widely known about and are difficult to access, being available only in large-scale research facilities like the ILL. In this article, we focus on recent work in the microelectronics sector.

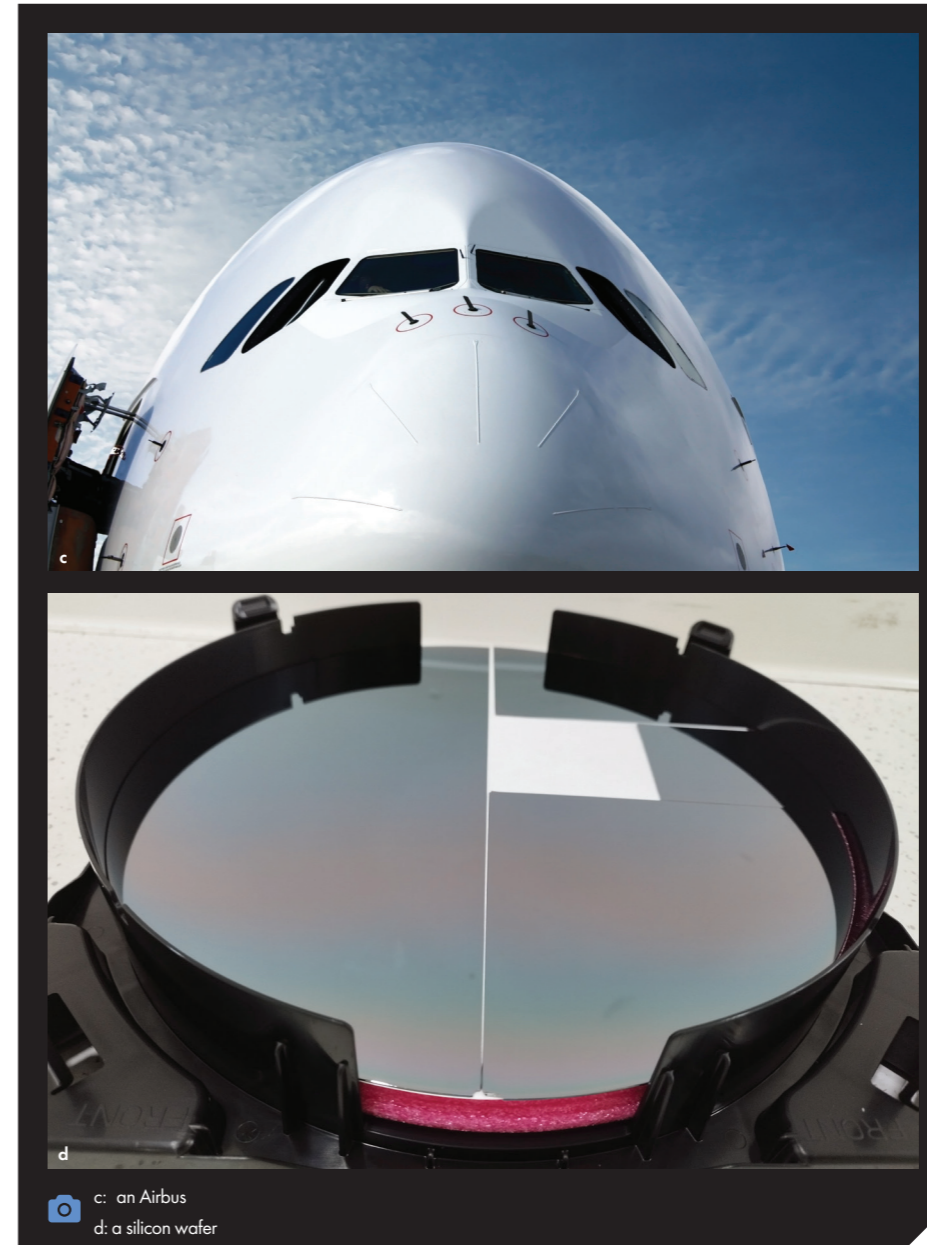
Recognising the need to bring research and industry closer together, developed economies have created organisations such as RTOs for this very purpose. In France, Technological Research Institutes (IRTs) are located in specific regions and focus on particular industry sectors. In Grenoble, 'The IRT-Nanoelec project' focuses on the microelectronics industry sector. Here, industry partners include STMicroelectronics and Schneider.

IRT-Nanoelec provides the ideal opportunity to explore the use of neutrons for the microelectronics industry. The ILL and ESRF have been partners since 2010. Initial funding investment at the ILL created the multi-purpose instrument D50 that was used for imaging, reflectometry and irradiation. D50 has subsequently been transformed into the dedicated imaging instrument NeXT, neutron-imaging being one of the most-used techniques by industry. In addition, irradiation capability has been created on the H9 beam line TENIS.

The relevance of electronic devices to society is abundantly clear—they are omnipresent. They are also taking on ever more sophisticated roles in our lives, increasingly involving artificial intelligence applications (for example, in self-driving vehicles) where the combination of hardware and software must be highly reliable. Both the ILL and IRT-Nanoelec are part of the EU infrastructure project, RADNEXT. The project supplies a network of facilities and irradiation methodologies for responding to the emerging needs of electronic component and system irradiation for optimising the radiation hardness. Thermal and high-energy neutrons are produced as a cascade of secondary particles in the Earth's atmosphere, causing Single-Event Upsets where the thermal neutrons interact with the boron-10 in devices.

The intense neutron beam on TENIS is ideal for accelerated testing. For example, DRAM memory has been tested in an extensive collaboration involving Infineon Technologies and ISIS for high-energy neutrons [1]. Given the rapid evolution towards artificial intelligence applications, there have been two notable studies on TENIS: one on the effects of thermal neutron radiation on a hardware-implemented Support Vector Machine learning algorithm [2]; the other, investigating the reliability impacts of neutron-induced soft errors in aerial image classification using convolutional neural networks [3].

Electronics are also used in very high



c: an Airbus
d: a silicon wafer



a: VR of TENIS – making the instrument/technique accessible
b: an electronic component (DRAM/FPGA/GPU/Raspberry Pi/...)

radiation environments. A particularly relevant example of this is the thermal neutron flux measurement at the particle accelerators at CERN which employ two radiation-tolerant, custom-measurement systems calibrated using the 'clean' thermal neutron beam on TENIS. A higher radiation environment also occurs at altitudes at which airplanes fly. The ILL is working with Airbus Avionics on a project to characterise the risks associated with thermal neutrons for avionics equipment by providing thermal neutron detectors to accurately measure neutron fluxes inside aircraft. More than 30 hours of in-flight tests were performed in 2021 and 2022. The neutron detectors were also tested at lower altitude as they made their return trip in the car to the local ski resort!

In another example, the microelectronics industry makes extensive use of silicon wafers. Silicon wafers can form part of stacked systems involving resins and protective coatings produced by photolithography. The performance of integrated circuits produced in this way depends on their purity and the diffusion of small molecules such as water through the layers. Neutron reflectometry, which can measure surfaces and interfaces on the nm scale and is particularly sensitive to molecules like water, is the ideal experimental technique for this work. Initial work on D17 [4] is now being extended to new applications.

Contributors:

Manon Letiche, Caroline Boudou, Duncan Atkins and Mark Johnson.

References:

- [1] Microelectronics Reliability (2022)– DOI: <https://doi.org/10.1016/j.microrel.2021.114406>
- [2] 27th IEEE International Conference on Electronics, Circuits and Systems (ICECS) (2020)–DOI: <https://doi.org/10.1109/ICECS49266.2020.9294938>
- [3] Microelectronics Reliability (2022)– DOI: <https://doi.org/10.1016/j.microrel.2022.114738>
- [4] Journal of Applied Physics 117 (2015)– DOI: <https://doi.org/10.1063/1.4921865>



More than simply neutrons

Scientific support laboratories

The ILL is firmly committed not only to building high-performance instruments, but also to offering the best possible scientific environment for its user community. Over the years, we have established several collaborations with neighbouring institutes and we have launched a number of successful scientific and support partnerships. Local collaboration is particularly important, which is why the three European institutes—the EMBL, the ESRF and the ILL—and France's IBS, have transformed their site into what is now the European Photon and Neutron (EPN) science campus, creating a veritable hub of international science in the Grenoble region. Find out more at <http://www.epn-campus.eu/>

Partnership for Soft Condensed Matter

The Partnership for Soft Condensed Matter (PSCM) is a joint initiative established by the ILL and the ESRF to strengthen the soft matter research community. The PSCM's main mission is to provide support services to ILL and ESRF scientists and users tackling contemporary challenges in soft matter research (nanomaterials, environmental and energy sciences, biotechnology and related fields). The PSCM offers a broad suite of equipment for preparing and characterising soft matter samples. For more information, visit the website <http://www.epn-campus.eu/pscm/>

Partnership for Structural Biology

The Partnership for Structural Biology (PSB) aims both to enhance the interdisciplinary capabilities of each of the facilities located on the EPN site and to widen the scientific scope of external user communities. It operates a powerful set of technology platforms that are provided and managed by its partner institutes. These platforms offer a host of advanced capabilities that complement the neutron scattering facilities available to ILL users: synchrotron X-rays, cryo-electron microscopy, high-field nuclear magnetic resonance, mass spectrometry and high-throughput methods as well as a range of biophysical techniques. For more information, visit the website <https://www.psb-grenoble.eu/>

The Deuteration Laboratory (D-Lab)

The Deuteration Laboratory (D-Lab) was created in the 2000s, with major funding from the UK's Engineering and Physical Sciences Research Council (EPSRC). Its principal missions are the provision of deuterated biomolecules to the user community, innovation and development for biological neutron scattering, and training.

D-Lab's user programme uses *in vivo* recombinant expression approaches to provide deuterated analogues of proteins, nucleic acids and lipids for the study of structure (crystallography, SANS, fibre diffraction, reflection) and dynamics using neutron scattering. The D-Lab is therefore of central importance to all the ILL instrument groups involved in biological research. In terms of development offers a broad range of activities, including novel deuteration regimes and the expression of deuterated proteins using mammalian cell deuteration, and provides expertise in the growth of large protein crystals.

There is no scheduled call for D-Lab proposal applications, which can be submitted at any time during the year. Access to the D-Lab is gained through a rapid peer-review proposal system and is open to all ILL member countries regardless of where the neutron scattering study is carried out. It is also available to users from non-member countries, although in such cases a contribution to the costs may be requested. Learn more at <https://www.ill.eu/D-Lab>

Chemistry Laboratories

The dual objectives of the Chemistry Laboratories are to provide ILL users with the option of preparing and characterising their samples during their neutron experiments, and to support the in-house research conducted by instrument scientists and PhD students.

The facilities comprise two sample preparation laboratories, a bio-preparation lab, a laboratory for handling corrosive substances, a balance room, an oven room and a cold room. The

sample preparation laboratories are equipped with fume cupboards, lab benches, demineralised and ultra-pure water, refrigerators, freezers and in-house gas lines (nitrogen, argon, compressed air). Standard lab equipment such as pH meters, balances, hot plates, stirrers, ultrasonic baths, centrifuges, automatic pipettes and a stock of glassware and basic chemicals are also provided. The oven room is equipped with standard ovens, vacuum ovens, a climate chamber and tube furnaces. A glovebox with an argon atmosphere and a fume cupboard for handling nano-powders are also available. Users can request access to the labs via the ILL User Club when registering for a scheduled experiment. Find out more at <https://www.ill.eu/users/support-labs-infrastructure/chemistry-laboratories/>

Materials Science Support Laboratory

The Materials Science Support Laboratory (MSSL) enables European materials engineers to make the best possible use of the advanced neutron and synchrotron X-ray facilities at the ILL and the ESRF. To that end, it supports a variety of materials engineering applications. New users can receive help with planning, conducting and evaluating their experiments, as well as with collecting, processing and analysing data. A full measurement and data analysis service is also available to industrial users, if required.

The MSSL has shared equipment for load testing (up to 50 kN), including a combined loading and heating device. It also provides facilities for sample polishing, hardness testing and optical microscopy. In addition, a Co-ordinate Measuring Machine (CMM) and a portable metrology arm are available for benchmarking sample surface dimensions and/or distortion before actual neutron measurements, making faster alignment of complex/large components possible directly at the beam line. Read more at <https://www.ill.eu/users/support-labs-infrastructure/materials-science-support-lab>

Platform for deuterated lipids (L-Lab)

The high levels of interest at the ILL in working with lipid bilayers—the major components of cellular membranes—and biological membranes is clear from the number of experiments performed (>200) and papers published (>300) on these topics over the past five years. There is also a growing interest among the user community in gaining access to deuterated glycerophospholipids (GPLs). GPLs are now the biomolecules most often requested by soft- and bio-neutron scientists.

While GPL deuteration helps to elucidate membrane structure, dynamics and function (by providing selective visualisation in neutron scattering), studies involving deuterated biomimetic membranes are currently limited by the low availability of these species. To overcome this, facilities such as the ANSTO and the ESS have been successful in chemically synthesising a small number of mono-unsaturated GPLs for users. An alternative and much cheaper method of obtaining a wide variety of deuterated GPL species is to extract them from microbes grown under deuterated conditions. The L-Lab at the ILL has therefore been set up specifically to cater for the needs of the user community by making natural deuterated GPL mixtures available.

Our facility puts strong emphasis on the development of novel lipid extraction and isolation techniques, focusing on: a) selecting and adapting suitable organisms for deuteration; b) optimising the extraction and separation of natural GPL mixtures; and c) reconstructing biologically relevant model membranes. In addition, we have made considerable efforts to characterise these GPL mixtures accurately, using various analytical and neutron scattering techniques in order to better understand the resulting lipid membranes. Consequently, deuterated GPL mixtures of this kind enable researchers to mimic natural bilayers for neutron scattering experiments.

This service was opened to users in February 2021. To find out more, visit <http://www.ill.eu/L-Lab>



Training and outreach

The ILL is committed to training and outreach, which it provides in many different forms. While the ILL Graduate School and PhD programme train future generations of neutron users, we also run neutron schools and other events for MSc and PhD students. In addition, our open days and annual contributions to the local science festival help attract young talent to science and improve the public's understanding of the science we perform.

The ILL Graduate School (IGS) has grown in strength over the past few years, as the ILL PhD programme has evolved and improved. It continues to provide training and financing for the equivalent of about 40 full-time, three-year PhD students from various ILL member countries. However, this number is scheduled to fall to 30 over the next couple years, due to budgetary constraints. The IGS also welcomes a number of PhD students with external funding.

A total of just nine ILL PhD students began their doctoral work in 2022, since there was no open call for PhD projects in autumn 2021. Nevertheless, the total number of active PhD students at the ILL, all funding schemes included, remains healthy thanks

partly to the 'second wave' of recruitment in 2021 via the InnovaXN PhD programme. This programme is financed by the EU through the Marie Skłodowska-Curie Actions COFUND programme. Its projects differ from the ILL's regular PhD projects in that each includes an industrial partner and, naturally, our InnovaXN projects have innovative industrial applications (hence the name). Other than extensive provision for PhD student courses and training (including transferable skills), an important aspect of the programme is that each InnovaXN student spends at least three months of internship working at the industrial partner's site during their PhD work.

We are happy to report that a total of 15 ILL PhD students successfully defended their doctoral work in 2022, and that there has been an autumn 2022 open call for new PhD projects.

The International Summer School for undergraduate students, organised by the ILL and the ESRF every year since 2014, allows undergraduate students from all our member countries to spend a month on site. Over the course of the four weeks, the students follow a series of lectures and seminars on the fundamentals and applications of X-rays, and work on a scientific project. The 2022 school, involving 22 students, was held from 4 to 30 September on the EPN campus.

The **Hercules School**, co-ordinated by the Université Grenoble Alpes and held every year since 1991, is a five-week course on neutron and synchrotron radiation for condensed matter studies for students and young scientists. The course includes lectures, hands-on practicals and tutorials in small groups, a poster session and visits to partner facilities including the ILL.

The 2022 session took place from 28 February to 1 April and attracted 135 applications. A total of 90 students were selected, representing some 33 nationalities and 21 countries. Although most of the participants were from Europe, there were also students from India, Iran, Mexico, Pakistan, Russia, Rwanda and Taiwan. The practicals and tutorials in Grenoble were held at the ILL, the ESRF, the CNRS and the CEA and/or the IBS. In all, participants attended about 85 hours of online lectures and 55 hours of online tutorials and practicals. Overall feedback on the school was extremely positive. More information is available at <https://hercules-school.eu/>

European collaborations

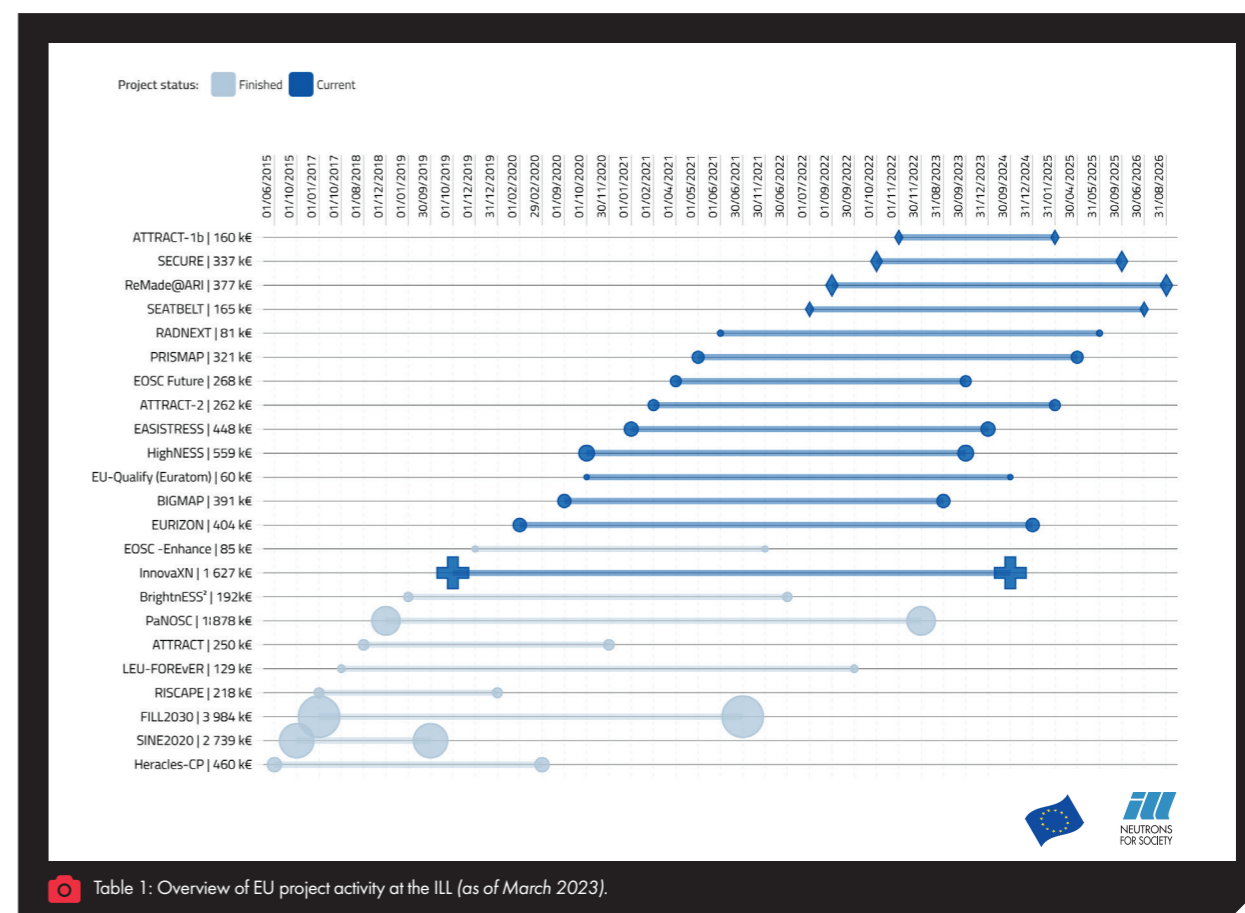


Table 1: Overview of EU project activity at the ILL (as of March 2023).

European collaboration has been part of the ILL's DNA since its inception. As the European Neutron Source the ILL has always been present on the European scene, be it through its co-ordination of and participation in European projects or the role it plays in EIROforum, the ESFRI and other European bodies. The ILL's activities at a European level help to ensure that Europe remains at the head of the field internationally.

Most of the ILL's project proposals are submitted in response to calls from the Horizon 2020 Research and Innovation programme, such as those relating to Research Infrastructures, the European Research Council, Marie-Sklodowska-Curie Action (MSCA), Euratom, Future and Emerging Technologies (FET) and Spreading Excellence and Widening Participation. Table 1 summarises EU project activity at the ILL.

The ILL is committed to training future generations of neutron users and to attracting young talents to science.



a: Welcoming the people of Grenoble to the ILL's booth during the local science festival, held in October every year. ©UtopikPhoto_PDS2022.
b: The ILL PhD students during their annual clip session



Workshops and events

ILL Chronicle 2022

17 February

LENS General Assembly.

7 March

Visit by Mrs Fraisse, CNRS Regional Delegate, and her deputy, Mrs Achin.

7 April

ILL Scientific Council.

5 May

EIROforum DG Assembly.

10–11 May

Meeting of the Subcommittee on Administrative Questions (SAQ).

16 June

Celebration of the 50th anniversary of the ILL's first neutrons.

23–24 June

Scientific Members' Meeting and Meeting of the ILL Steering Committee in Vienna (to celebrate 30+ years of Austria as a scientific member of the ILL).

4 July

Visit/seminar by Mr Brown, Los Alamos National Laboratory.

5 July

Visit by Mr Balzaretti, Swiss Ambassador, accompanied by delegations from the Swiss Embassy in Paris and the Swiss Consulate in Lyon.

6 July

Visit by Consul General Mr Pröpstl, German Consulate in Lyon.

29 August

Visit by Mr Sakhiyev, Director of the Institute of Nuclear Physics in Kazakhstan; and by Mr A. Shaimerdenov, accompanied by Mr Nessibkulov, from the Embassy of Kazakhstan in Paris.

6 September

Visit by Mr Harrison, Diamond Light Source, accompanied by two visitors from CERIC-ERIC.

7 September

Visit by Mrs Forrester-Sotto, Head of the School of Life Sciences, Keele University.

9 September

Meeting of the Associates, in Grenoble.

12 September

Strategy post-2023 workshop at the German Embassy in Paris, and 3rd meeting of the 'Strategy Working Group'.

11–12 October

Meeting of the Subcommittee on Administrative Questions (SAQ).

24 October

Visit by Mr Brandenburg, the German state secretary for research and education.

28 October

Extraordinary Meeting of the Subcommittee on Administrative Questions (SAQ).

7–10 November

Subcommittee and ILL Scientific Council meetings.

24–25 November

Meeting of the ILL Steering Committee.

28 November

Visit by Mr Dauxois, Director of the Physics Institute/CNRS, accompanied by three INP scientific deputy directors.

14 December (tbc)

Visit by Mr Piolle, Mayor of Grenoble, accompanied by Mrs Barnola, Director of the Mayor's Cabinet, and Mr Reval, Associate Director.



a: 30+ years' Austrian Membership of the ILL. © E. Zilberberg-ÖAW

b: Strategy post-2023 workshop at the German Embassy in Paris, 12 September. © German Embassy.

c: Subcommittee meetings, 7–8 November.

d: Meeting of the ILL Steering Committee, 24 November.

e: Visit of the German state secretary for research and education, Mr Mario Brandenburg (second from left), 24 October.

f: Visit by Mr Eric Piolle, Mayor of Grenoble (third from right).

Scientific events

In 2022, the ILL organised (or co-organised) 15 scientific events (workshops, conferences and schools). In the same year, a total of 50 general seminars were organised at the ILL, in addition to 3 colloquia.

Workshops

17 May

Foam-scatter: a workshop on foam characterisation.

18–20 May

The Extraordinary Structure of Ordinary Things. A tribute to Isabelle Grillo.

1–3 June

EIROforum workshop—Robotics & Remote Operation.

20–24 June

European Molecular Biology Organisation (EMBO).

2 September

Instrument review.

11–15 September

DYNAFUN—Dynamics of Functional Materials.

20–22 September

Easi-STRESS project meeting.

25–28 September

50 years of D11—A history of SANS at the ILL.

5–7 October

ESS/ILL User Meeting in Lund.

11–13 October

CONFIT—5th international workshop on Dynamics in Confinement.

16–21 October

ADD2022—Analysis of Diffraction Data in Real Space.

2–4 November

Perspectives on High-Magnetic Fields at Neutron Sources.

Schools

28 February–1 April

HERCULES European School

20–28 June

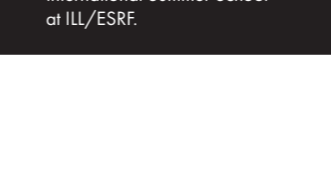
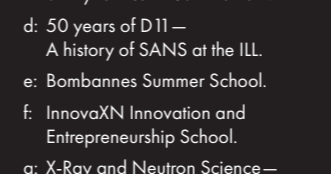
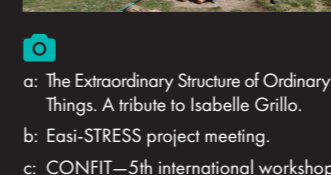
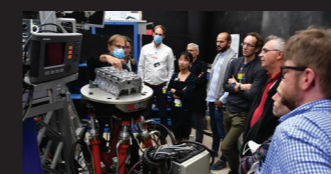
Bombannes Summer School

4–30 September

X-Ray and Neutron Science—International Summer School at ILL/ESRF

15–18 November

InnovaXN Innovation and Entrepreneurship School



a: The Extraordinary Structure of Ordinary Things. A tribute to Isabelle Grillo.

b: Easi-STRESS project meeting.

c: CONFIT—5th international workshop on Dynamics In Confinement.

d: 50 years of D11—A history of SANS at the ILL.

e: Bombannes Summer School.

f: InnovaXN Innovation and Entrepreneurship School.

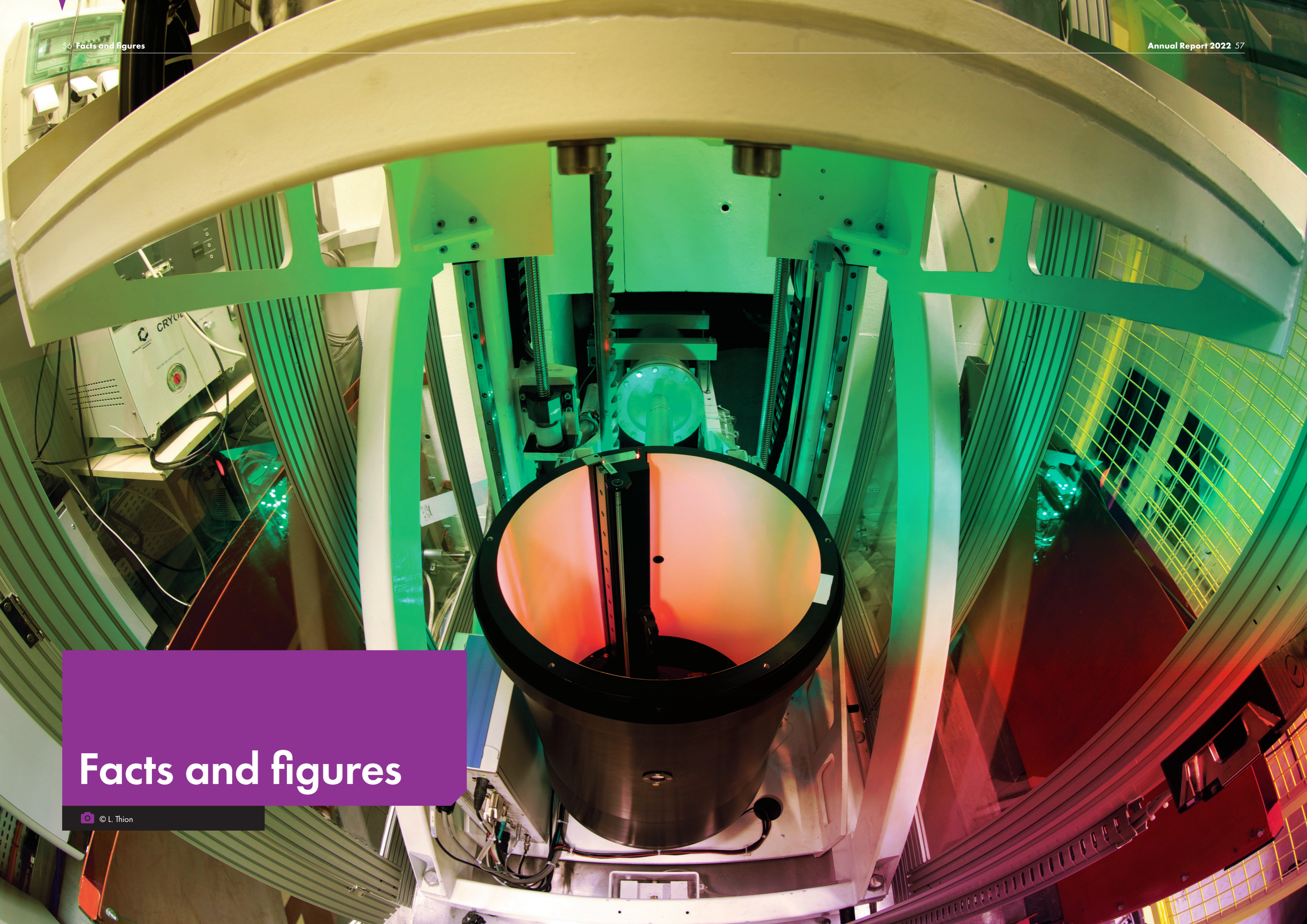
g: X-Ray and Neutron Science—International Summer School at ILL/ESRF.

On 16 June, the ILL celebrated the 50th anniversary of the first divergence of the reactor.



Facts and figures

© L. Thion



Key figures in 2022

Publications:

600

ILL publications recorded in 2022 of which **145** published in high-impact journals

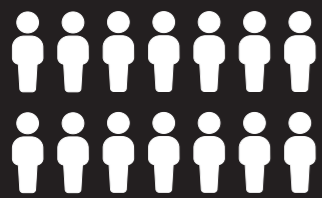
Industrial use:

106 companies since 2011

26 measurement periods

Revenue: **506 k€**

14 unique customers



108 M€ annual income:

73 % from the Associates and 19 % from Scientific Member countries

536 members of staff

of **32** different nationalities

Reactor power

58.3 MW Flux 1.5×10^{15} n/s cm²

A single highly enriched uranium fuel element

Training:

Graduate School
40 full-time-equivalent ILL PhD Students

HERCULES School
90 participants of **33** different nationalities working in **21** different countries

Events:

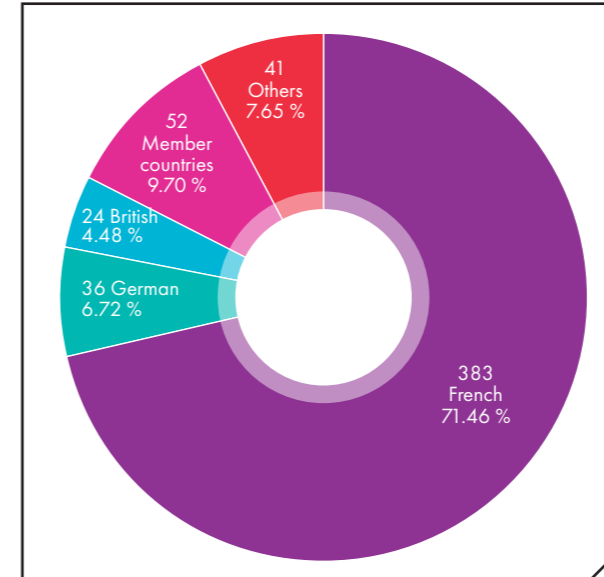
15 scientific events workshops, schools and conferences

50 general seminars and **3** colloquia

Staff on 31 December 2022

The ILL employs 536 people, including 73 experimentalists in the scientific sector and 49 thesis students.

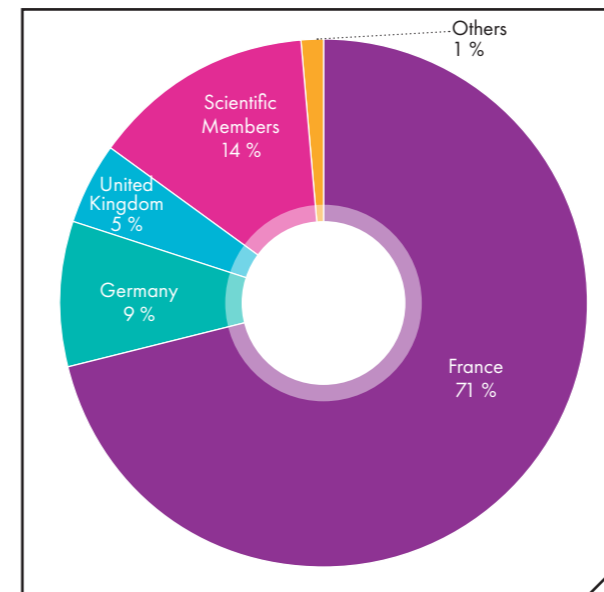
In total, they comprise 32 different nationalities: 383 French; 36 German; 24 British; 52 Member countries; and 41 others.



Distribution of ILL staff by nationality (number and %)



Gender balance per area of activity (total share of women 27.29 %)

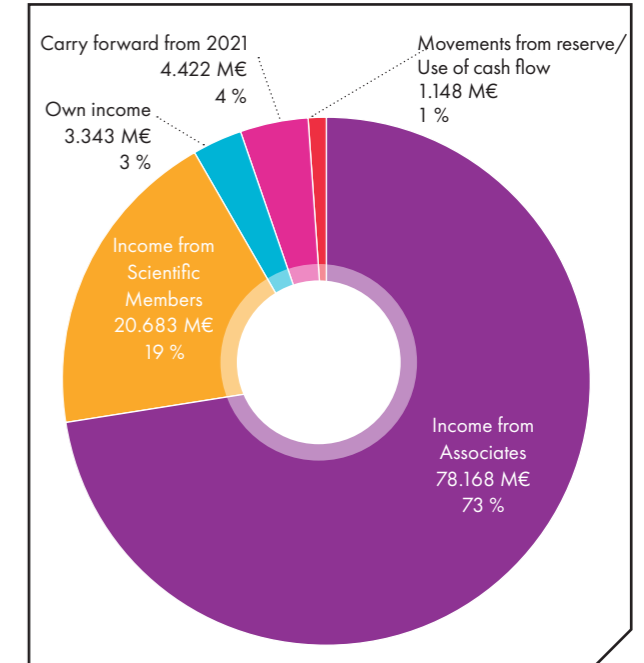


Purchasing statistics – non-captive market

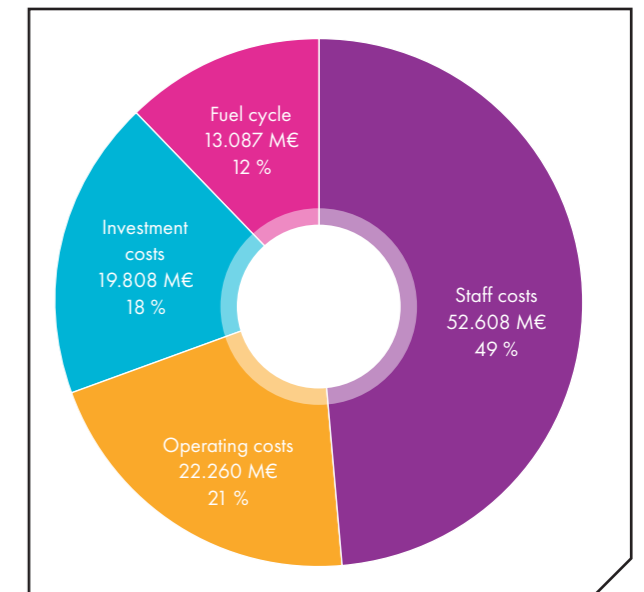
Implementation budget 2022: 107.764 M€ (excluding taxes)

The ILL's Associate countries (France, Germany and the UK) contributed some 78 M€ to the Institute in 2022, a sum enhanced by significant contributions from the ILL's Scientific Member countries. The contribution of the Associates covers the Endurance Programme, additional nuclear taxes and insurance.

The ILL's overall budget in 2022 amounted to about 108 M€.



Income budget: contributions (in M€ and %)



Expenditure: (in M€ and %)

Name

Institut Max von Laue-Paul Langevin (ILL).

Founded

19 January 1967.

Intergovernmental Convention between France, Germany and the United Kingdom (19/07/1974).

Supervisory and advisory bodies

Steering Committee, which meets twice a year.

Subcommittee on Administrative Questions, which meets twice a year.

Audit Commission, which meets once a year, and statutory auditor.

Scientific Council with 9 Subcommittees, which meets twice a year.

Review panels – January 2023**Key Chair/focus group Chair**

ILL college secretary/focus group secretary

Applied metallurgy, instrumentation and techniques

M. Strobl (PSI, Switzerland)

L. Helfen

Nuclear and particle physics

G. Pignol (LPSC, France)

C. Michelagnoli

Magnetic excitations

H. Walker (STFC, UK)

U.B. Hansen

Crystallography

M. Widenmeyer (TU Darmstadt, Germany)

O. Fabelo

Magnetic structures

A. Gibbs (ISIS, UK)/

D. Lott (GKSS Forschungszentrum, Germany)

A. Rodríguez Velamázan/N. Steinke

Structure and dynamics of liquids and glasses

D. Morineau (University of Rennes, France)

M. Appel

Spectroscopy in solid state physics and chemistry

F. Juranyi (PSI, Switzerland)

J. Ollivier

Structure and dynamics of biological systems

J.R. Lu (University of Manchester, UK)

O. Matsarskaia

Structure and dynamics of soft condensed matter

E. Dubois (Pierre and Marie Curie University, Paris, France)/

R. Campbell (University of Manchester, UK)

O. Czakkal/L. Chiappisi

Associates**France**

Commissariat à l’Energie Atomique et aux Energies Alternatives (CEA)

Centre National de la Recherche Scientifique (CNRS)

Germany

Forschungszentrum Jülich (FZJ)

United Kingdom

United Kingdom Research & Innovation (UKRI)

Countries with Scientific Membership

Spain: MCIN Ministerio de Ciencia e Innovación

Switzerland: Staatssekretariat für Bildung, Forschung und Innovation (SBFI)

Italy: Consiglio Nazionale delle Ricerche (CNR)

Belgium: Belgian Federal Science Policy Office (BELSPOL)

Sweden: Swedish Research Council (VR)

Denmark: Danish Agency for Science and Higher Education

Poland: (NDPN) Consortium of Polish Scientific and Research Institutions

Slovenia: The Slovenian National Institute of Chemistry

CENI (Central European Neutron Initiative)

Consortium composed of:

Austria: Österreichische Akademie der Wissenschaften

Czech Republic: Charles University, Prague

Slovakia: Comenius University, Bratislava

Contractually agreed beamtime**share for Member countries**

Austria	2.500 %	
Czech Republic	0.750 %	
Slovakia	0.184 %	
Belgium	0.550 %	
Sweden	4.500 %	
Denmark	1.570 %	
Italy	1.300 %	
Switzerland	2.372 %	average over 5 years
Spain	4.500 %	average over 5 years
Poland	0.800 %	
Slovenia	0.150 %	

Reactor

No reactor cycles were scheduled in 2022.

A long reactor shut down, from October 2021 to February 2023, was necessary to carry out important work. This included replacing the H1–H2 beam tube and carrying out most of the remaining Endurance projects, as well as performing a lot of the work to which the ILL is committed for the French Nuclear Safety Authority, ASN.

Publications in 2022

In 2022, the ILL received notice of **600** publications, **145** of which were published in high-impact journals.

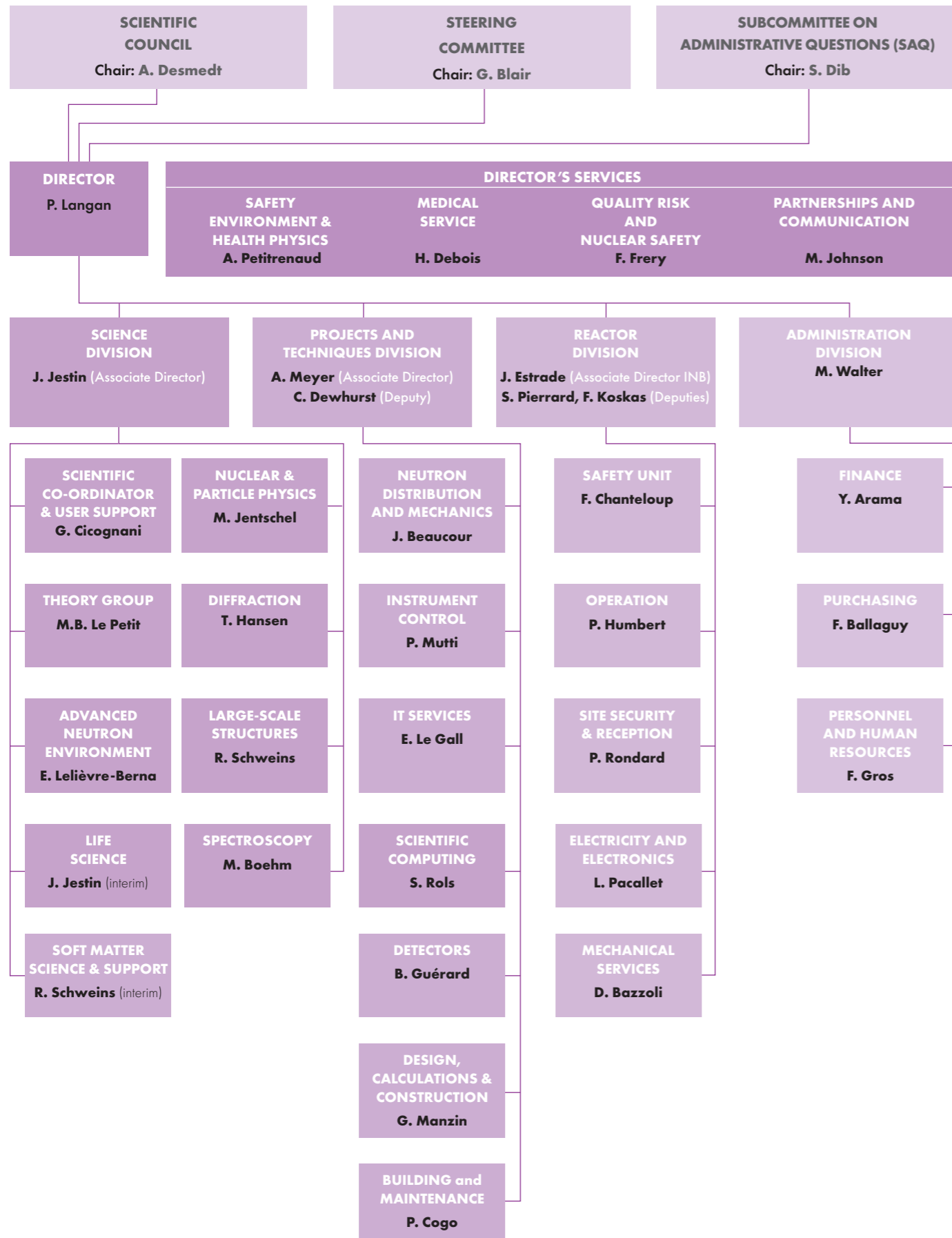
Biology	61
Liquids and Glasses	22
Applied Physics, Instrumentation and Techniques	45
Nuclear and Particle Physics	63
Soft Matter	106
Theory	16
Magnetic Excitations	35
Magnetic Structures	96
Spectroscopy in Solid State Physics and Chemistry	30
Materials Science and Engineering	54
Crystallography and Chemistry	67
Medicine	5

ILL PhD Studentships

Full-time-equivalent ILL-funded PhD projects in 2022	40
PhD students working on ILL PhD projects in 2022	60*
Successfully defended ILL PhD theses in 2022	15

*includes PhD projects that are co-funded or completely externally funded

A long reactor shut down, from October 2021 to February 2023, was necessary to carry out important work.



71, avenue des Martyrs
38000 Grenoble
France
www.ill.eu



This report has been printed using FSC certified paper www.fsc.org